Doctoral Dissertation

Precise Control of Thermo-responsive Properties of OEG-alkanethiol Modified Gold Nanoparticles

（OEGを有するアルカンチオールで修飾した金ナノ粒子の温度応答性の精密制御）

Kun Xiong

Doctor of Soft Matter Science

Graduate School of Life Sciences,

Hokkaido University

March 2023

Contents

Chapter 1

General Introduction

1-1. Optical properties of gold nanoparticles

Compared to bulk one, nanoparticles with smaller sizes (1~100 nm) show larger surface to volume ratio increasing their chemical reactivity, catalytic activity, stability in suspension.[1] Gold nanoparticles (AuNPs) is a widely used nanoparticles that show biocompatible,[2] and optical properties such as localized surface plasmon resonance (LSPR) under visible light irradiation. LSPR is a phenomenon that the free electrons of the AuNP oscillate coherently with the oscillating electromagnetic field of the incident light, enhancing the electromagnetic field at the AuNP surface and accompanying the maximum optical absorption at this plasmon resonant frequency (Figure 1-1A, B).[3,4] Electromagnetic field enhanced by LSPR provides the enhancement of the Raman scattered light of molecules near the AuNPs, called a surface-enhanced Raman scattering (SERS),[5–7] and it is used for applications to target tumors and provide detection in vivo.[8] Optical absorption causes the heat generation from the AuNPs by photothermal conversion, and it is expected to be applied for thermophotovoltaics.[9]

The shape and the size of AuNP have a great effect on optical properties. Tuning of AuNP's size provide the direct control of the maximum optical absorption by LSPR.[10] On the other hand, the anisotropic AuNPs with various morphologies (nanorod,[11–13] triangular nanoplate,[14–16] nanocube,[17,18] and so on) also show different plasmon absorption.[19] The well-known rod-shaped gold nanoparticles (AuNRs) perform two kinds of LSPR corresponding to a transverse and longitudinal LSPR (Figure 1-1C).[20] The peak of longitudinal LSPR can be tuned from the visible to the near infrared (NIR) region by control of the aspect ratio.[21,22] Since NIR light transmits readily through human skin and tissue, AuNRs are promising to be used for the photothermal cancer therapy, which kills tumor cells via heat produced by NIR light photothermal conversion.[23–25] Nevertheless,

this therapy damages not only tumor tissues but also normal tissues and supposed to cause the new health problems (Figure 1-1D). In addition, the size of AuNRs exceeding the renal excretion threshold is also a problem.[26,27] To improve the selectivity and biocompatibility of this treatment, control of assembly of gold particles at some time in someplace is a research direction.

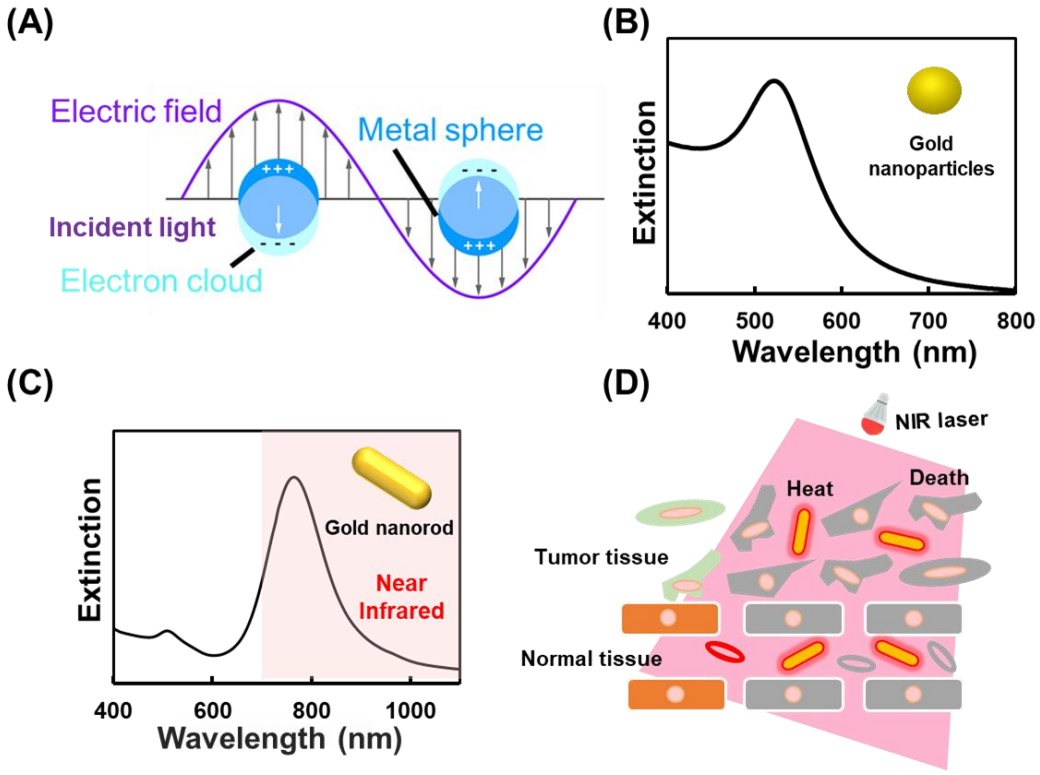

Figure 1-1. (A) An illustration of localized surface plasmon resonance (LSPR); Plasmon absorption by LSPR: (B) Gold nanoparticles (AuNPs); (C) Gold nanorods (AuNRs). (D) Photothermal cancer therapy using AuNRs

1-2. Assembly of gold nanoparticles

Individual nanoparticles automatically form an organized pattern or structure without human intervention is called "self-assembly". Assembly of nanoparticles can express novel functions that are different from those displayed by individual nanoparticles and the bulk state. Precise and ordered nanostructures such as vesicles[28–31] fabricated via self-assembly of AuNPs show the functions of drug delivery carriers.[32,33] Importantly, the new optical properties also generate due to this self-assembly. For instance, it causes the adjacent nanoparticles approaching to each other, resulting in the plasmon peak shift to the near-infrared area due to interparticle plasmon coupling corresponding to hybrids of the LSPR of individual particles (Figure 1-2A).[34,35] The absorption of NIR light suggest assemblies of AuNPs can be applied to photothermal cancer therapy. Furthermore, the differences in properties before and after assembly are supposed to perform the properties selectively by control of the assembly of nanoparticles. Different from non-selective AuNRs, assemblies of AuNPs in tumor tissues and individual dispersed AuNPs in normal should be a good method to targeted photothermal cancer therapy. As well-known, the body temperature of tumor tissues are higher than normal tissues.[36] Thermo-responsive assemblies of AuNPs only in tumor tissue is expected to achieve a desired therapeutic effect at target site and reduce the damage to normal tissues. To control this thermo-responsive assembly, introducing the interaction to the adjacent particles is necessary. Surface modification with ligand molecules is an effective method to provide such interaction.

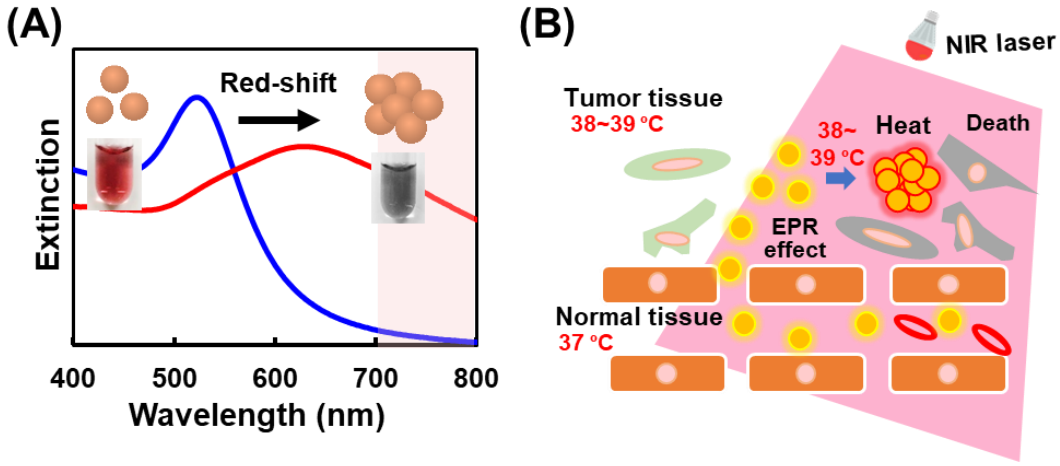

Figure 1-2. (B) Plasmon absorption before (blue) and after (red) assembly of AuNPs; (B) Photothermal cancer therapy using assemblies of AuNPs

1-3. Surface modification

Surface modification plays an important role to provide the desired surface properties to AuNPs. For instance, ethylene glycol-connected molecules and oligo and poly(-ethylene glycol) (OEG and PEG), which show good water-solubility and biocompatibility, are attached to nanoparticles to improve their dispersibility and retentivity in blood during medical and therapeutic applications.[37–39] Importantly, surface modification with stimuli-responsive ligand molecules induce self-assembly/disassembly of gold nanoparticles in response to various stimulus, such as temperature.[40–45] These thermo-responsiveness are based on the fact that the AuNPs disperse at a certain temperature due to hydration of ligand molecules and assemble at other certain temperature due to dehydration resulting in the hydrophobic interaction between adjacent ligand molecules.

To date, synthetic polymers, such as poly(N-isopropylacrylamide) (pNIPAM), are widely used as thermo-responsive ligands due to phase transition over lower critical solution temperature (LCST),[46–52] resulting in assembly of gold nanoparticles. Furthermore, to ensure ligands binding with AuNPs firmly, the functional group -thiol is attached to the ligand to provide the robust Au-S bond and its binding energy is ~40 kJ/mol.[53,54] Nevertheless, there are still some issues in control of this thermo-responsive assembly. Firstly, polydisperse in synthetic polymers are supposed to cause a variety of conformation and configuration on AuNP surface, probably resulting in broadening surface properties. Secondly, the large molecular sizes of polymers determine the thickness of surface coating, leading to the large interparticle gaps on nanoparticle assembly. The large gaps will weaken the intensity of plasmon coupling of gold nanoparticles. In addition, it has been reported that nanoparticles modified with polymer

show constant assembly temperature (T_A) independent ligand density, which is considered as an important factor in determining the thermo-responsive property since local ligand density influence dehydration.[52] Although the stable T_A is a merit in some applications, it is poor to program the thermo-responsiveness using control of ligand density. On the other hand, alkanethiol ligands have attracted much attention due to their uniform structure and size. Compared to polymer, alkanethiols can form highly packed and ordered self-assembled monolayer leading to their uniform conformation (Figure 1-3A). [55] The small molecule of alkanethiols result in the thin thickness. Furthermore, OEG-attached alkanethiols show the bio-compatible and thermo-responsive properties.[56] AuNPs modified with OEG-alkanethiol showed assembly/disassembly due to dehydration/hydration of OEG portion in ligands at a certain temperature (T_A) (Figure 1-3B).[57] Our group have reported that the T_A drastically changed along with the change in hydrophobic terminus in OEG-alkanethiols and the core size of gold nanoparticles corresponding to the local density of OEG-alkanethiols, suggesting the controllable thermo-responsiveness on local ligand density and terminal hydrophobicity.[58] For bio-application, precise control of thermo-responsiveness is required.

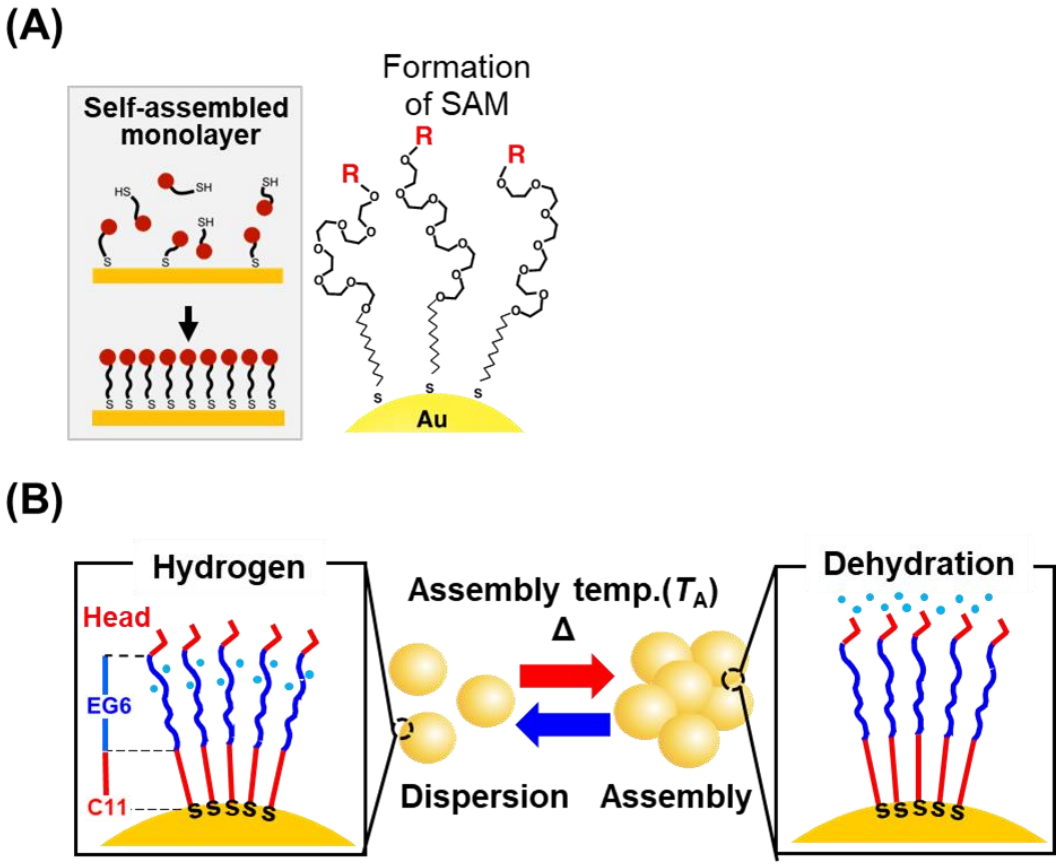

Figure 1-3. (A) An illustration of immobilize ligand molecules on AuNPs forming a self-assembled monolayer (SAM); (B) Disassembly/assembly of AuNPs due to hydration/dehydration of OEG-alkanethiols

1-4. Precise control of thermo-responsiveness

For instance, to realize tumor-targeted photothermal cancer therapy, the gold nanoparticles only assemble at the body temperature in tumor tissues which is 1~2 ºC higher than that in normal tissues, suggesting the assembly temperature should be tuned around body temperature of tumor tissues accurate to less than 1 ºC. In other words, the precise control of thermo-responsiveness is necessary in bio-application. However, it is not so easy. Although the OEG-alkanethiol modified AuNPs show the controllable thermo-responsiveness, tiny change in hydrophobic terminus of alkanethiol ligands and core size of AuNPs corresponding to the local OEG density result in drastic change in T_A (Figure 1-4),[58] which is not suitable for bio-application. It can be explained that these are the slight changes in structure and local density of ligands, but the accumulation of these changes from this kind of ligand in highly packed and ordered SAMs lead to the change in local environment and configuration of ligands, resulting in the drastic change in T_A. Additionally, there are some reports that surface modification with mixed ligand molecules resulted in AuNPs obtain the hybrid surface properties and structure from these ligands.[59–62] That is expected to tune T_A at between two kinds of OEG-alkanethiol ligands by surface modification with these mixed ligands. Furthermore, now that AuNPs are modified with a mixture of two kinds of ligands, the bias in surface modification has to be considered for precise control of thermo-responsiveness.

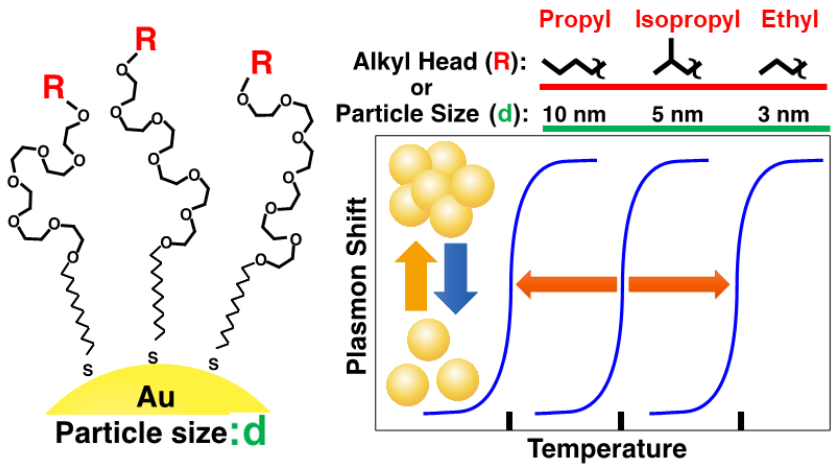

Figure 1-4. Assembly temperature of AuNPs changed along with the changes in hydrophobic terminus in alkanethiol ligands and core sizes of AuNPs

1-5. Objective

Gold nanoparticles (AuNPs) show localize surface plasmon resonance (LSPR), which accompanies with light absorption and heat production. The anisotropic gold nanorods (AuNRs) show a strong plasmon absorption in near infrared (NIR) region and are expected to be applied to photothermal cancer therapy. However, the damages to normal tissues and size exceeding the renal excretion threshold are still problems. On the other hand, assemblies of AuNPs also show the plasmon absorption of NIR light. Importantly, thermo-responsive assembly of AuNPs selectively in tumor tissues with higher body temperature should be a good method to tumor-targeted therapy. OEG-alkanethiols ligands were used to surface modify the AuNPs to provide the thermo-responsiveness. The assembly temperature (T_A) drastically changed along with the changes in hydrophobic terminus of alkanethiols and core size of AuNPs. For bio-application, precise control of thermo-responsiveness is required. Thus, in this study, I focused on the surface modification to precisely control thermo-responsiveness. (Figure 1-5).

Chapter 2, I precisely tuned the T_A of AuNPs by surface modification with mixed OEG-alkanethiol ligands based on the local environmental control not only by the hydrophobic terminus of alkanethiol ligands but also by core size of AuNPs influencing the thermo-responsiveness. Firstly, I modified AuNPs using the mixed ligands of two kinds of thermo-responsive OEG-alkanethiol with different hydrophobic terminus to control the surface hydrophobicity, resulting in tuning T_A at between these two ligands. Further, although precise size control is difficult, I tuned the T_A by the ligand mixing with a non-thermo-responsive ligand with a shorter OEG length to control the local OEG density to reach the core size effect.

Chapter 3, I investigated the factors leading to the biased surface modification and supported the precise control of thermo-responsiveness by fair surface modification. In this study, ligand exchange can be the one of the reasons of bias surface modification. Therefore, firstly, I confirmed the ligand exchange by addition of the free alkanethiols ligand to alkanethiols modified AuNPs to observe the change in thermo-responsiveness. Next, kinetic analyses of ligand exchange on time course experiment was performed to investigate how ligand exchange proceed and give the effect on the surface modification. Finally, based on the investigation of ligand exchange, I preformed the surface modification carefully and tried to restrain the bias in surface modification.

Chapter 4, I summarize the thesis and afford the significance and prospects.

Chapter 2 ***Precise Control of Thermo-responsiveness of AuNPs by Surface Modification with Mixed Ligand***

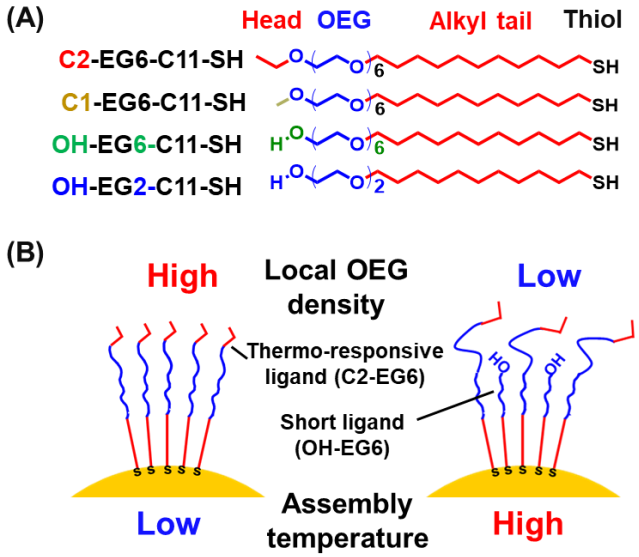

Chapter 3 ***Well-control of Ligand Exchange for Fair Surface Modification***

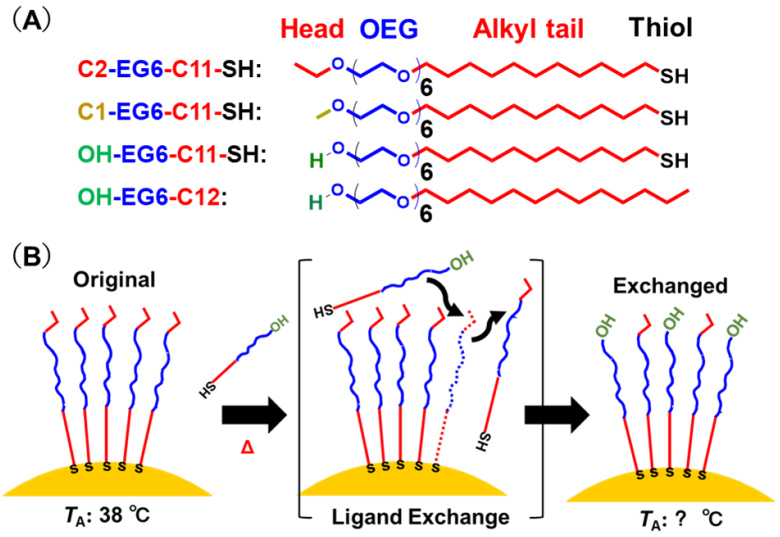

Figure 1-5. Schematic illustration of my doctoral thesis.

1-5. Reference

(1) Sajanlal, P. R.; Sreeprasad, T. S.; Samal, A. K.; Pradeep, T. Anisotropic Nanomaterials: Structure, Growth, Assembly, and Functions. *Nano Rev.* **2011**, *2* (1), 5883.

(2) Liu, R. R.; Song, L. T.; Meng, Y. J.; Zhu, M.; Zhai, H. L. Study on Biocompatibility of AuNPs and Theoretical Design of a Multi-CDR-Functional Nanobody. *J. Phys. Chem. B* **2019**, *123* (35), 7570–7577.

(3) Willets, K. A.; Van Duyne, R. P. Localized Surface Plasmon Resonance Spectroscopy and Sensing. *Annu. Rev. Phys. Chem.* **2007**, *58* (1), 267–297.

(4) Sinha, S. S.; Paul, D. K.; Kanchanapally, R.; Pramanik, A.; Chavva, S. R.; Viraka Nellore, B. P.; Jones, S. J.; Ray, P. C. Long-Range Two-Photon Scattering Spectroscopy Ruler for Screening Prostate Cancer Cells. *Chem. Sci.* **2015**, *6* (4), 2411–2418.

(5) Pazos-Pérez, N.; Ni, W.; Schweikart, A.; Alvarez-Puebla, R. A.; Fery, A.; Liz-Marzán, L. M. Highly Uniform SERS Substrates Formed by Wrinkle-Confined Drying of Gold Colloids. *Chem. Sci.* **2010**, *1* (2), 174–178.

(6) Chen, G.; Wang, Y.; Yang, M.; Xu, J.; Goh, S. J.; Pan, M.; Chen, H. Measuring Ensemble-Averaged Surface-Enhanced Raman Scattering in the Hotspots of Colloidal Nanoparticle Dimers and Trimers. *J. Am. Chem. Soc.* **2010**, *132* (11), 3644–3645.

(7) Joseph, V.; Engelbrekt, C.; Zhang, J.; Gernert, U.; Ulstrup, J.; Kneipp, J. Characterizing the Kinetics of Nanoparticle-Catalyzed Reactions by Surface-Enhanced Raman Scattering. *Angew. Chemie - Int. Ed.* **2012**, *51* (30), 7592–7596.

(8) Qian, X.; Peng, X. H.; Ansari, D. O.; Yin-Goen, Q.; Chen, G. Z.; Shin, D. M.; Yang, L.; Young, A. N.; Wang, M. D.; Nie, S. In Vivo Tumor Targeting and Spectroscopic Detection with Surface-Enhanced Raman Nanoparticle Tags. *Nat. Biotechnol.* **2008**, *26* (1), 83–90.

(9) ElKabbash, M.; Sousa-Castillo, A.; Nguyen, Q.; Mariño-Fernández, R.; Hoffman, N.; Correa-Duarte, M. A.; Strangi, G. Tunable Black Gold: Controlling

the Near-Field Coupling of Immobilized Au Nanoparticles Embedded in Mesoporous Silica Capsules. *Adv. Opt. Mater.* **2017**, *5* (21), 1–6.

(10) Navarro, J. R. G.; Lerouge, F. From Gold Nanoparticles to Luminescent Nano-Objects: Experimental Aspects for Better Gold-Chromophore Interactions. *Nanophotonics* **2017**, *6* (1), 71–92.

(11) Park, H. S.; Agarwal, A.; Kotov, N. A.; Lavrentovich, O. D. Controllable Side-by-Side and End-to-End Assembly of Au Nanorods by Lyotropic Chromonic Materials. *Langmuir* **2008**, *24* (24), 13833–13837.

(12) Chen, H.; Shao, L.; Li, Q.; Wang, J. Gold Nanorods and Their Plasmonic Properties. *Chem. Soc. Rev.* **2013**, *42* (7), 2679–2724.

(13) Wang, G.; Akiyama, Y.; Kanayama, N.; Takarada, T.; Maeda, M. Directed Assembly of Gold Nanorods by Terminal-Base Pairing of Surface-Grafted DNA. *Small* **2017**, *13* (44), 1–8.

(14) Zhai, Y.; DuChene, J. S.; Wang, Y. C.; Qiu, J.; Johnston-Peck, A. C.; You, B.; Guo, W.; Diciaccio, B.; Qian, K.; Zhao, E. W.; et al. Polyvinylpyrrolidone-Induced Anisotropic Growth of Gold Nanoprisms in Plasmon-Driven Synthesis. *Nat. Mater.* **2016**, *15* (8), 889–895.

(15) Kuttner, C.; Mayer, M.; Dulle, M.; Moscoso, A.; López-Romero, J. M.; Förster, S.; Fery, A.; Pérez-Juste, J.; Contreras-Cáceres, R. Seeded Growth Synthesis of Gold Nanotriangles: Size Control, SAXS Analysis, and SERS Performance. *ACS Appl. Mater. Interfaces* **2018**, *10* (13), 11152–11163.

(16) Scarabelli, L.; Coronado-Puchau, M.; Giner-Casares, J. J.; Langer, J.; Liz-Marzán, L. M. Monodisperse Gold Nanotriangles: Size Control, Large-Scale Self-Assembly, and Performance in Surface-Enhanced Raman Scattering. *ACS Nano* **2014**, *8* (6), 5833–5842.

(17) Skrabalak, S. E.; Au, L.; Li, X.; Xia, Y. Facile Synthesis of Ag Nanocubes and Au Nanocages. *Nat. Protoc.* **2007**, *2* (9), 2182–2190.

(18) Cortie, M. B.; Liu, F.; Arnold, M. D.; Niidome, Y. Multimode Resonances in Silver Nanocuboids. *Langmuir* **2012**, *28* (24), 9103–9112.

(19) Reguera, J.; Langer, J.; Jiménez De Aberasturi, D.; Liz-Marzán, L. M. Anisotropic Metal Nanoparticles for Surface Enhanced Raman Scattering. *Chem. Soc. Rev.* **2017**, *46* (13), 3866–3885.

(20) Cao, J.; Sun, T.; Grattan, K. T. V. Gold Nanorod-Based Localized Surface Plasmon Resonance Biosensors: A Review. *Sensors Actuators, B Chem.* **2014**, *195*, 332–351.

(21) Vigderman, L.; Khanal, B. P.; Zubarev, E. R. Functional Gold Nanorods: Synthesis, Self-Assembly, and Sensing Applications. *Adv. Mater.* **2012**, *24* (36), 4811–4841.

(22) Lohse, S. E.; Murphy, C. J. The Quest for Shape Control: A History of Gold Nanorod Synthesis. *Chem. Mater.* **2013**, *25* (8), 1250–1261.

(23) Song, J.; Pu, L.; Zhou, J.; Duan, B.; Duan, H. Biodegradable Theranostic Plasmonic Vesicles of Amphiphilic Gold Nanorods. *ACS Nano* **2013**, *7* (11), 9947–9960.

(24) Mackey, M. A.; Ali, M. R. K.; Austin, L. A.; Near, R. D.; El-sayed, M. A. The Most Effective Gold Nanorod Size for Photothermal Therapy - Seedless Growth.Pdf. **2014**.

(25) Song, J.; Yang, X.; Jacobson, O.; Huang, P.; Sun, X.; Lin, L.; Yan, X.; Niu, G.; Ma, Q.; Chen, X. Ultrasmall Gold Nanorod Vesicles with Enhanced Tumor Accumulation and Fast Excretion from the Body for Cancer Therapy. *Adv. Mater.* **2015**, *27* (33), 4910–4917.

(26) Cassano, D.; Pocoví-Martínez, S.; Voliani, V. Ultrasmall-in-Nano Approach: Enabling the Translation of Metal Nanomaterials to Clinics. *Bioconjug. Chem.* **2018**, *29* (1), 4–16.

(27) Vlamidis, Y.; Voliani, V. Bringing Again Noble Metal Nanoparticles to the Forefront of Cancer Therapy. *Front. Bioeng. Biotechnol.* **2018**, *6* (OCT), 1–5.

(28) He, J.; Liu, Y.; Babu, T.; Wei, Z.; Nie, Z. Self-Assembly of Inorganic Nanoparticle Vesicles and Tubules Driven by Tethered Linear Block Copolymers. *J. Am. Chem. Soc.* **2012**, *134* (28), 11342–11345.

(29) Kotov, N. A. As Protein Mimics. *Science* **2010**, *330*, 188–189.

(30) Niikura, K.; Iyo, N.; Higuchi, T.; Nishio, T.; Jinnai, H.; Fujitani, N.; Ijiro, K. Gold Nanoparticles Coated with Semi-Fluorinated Oligo(Ethylene Glycol) Produce Sub-100 Nm Nanoparticle Vesicles without Templates. *J. Am. Chem. Soc*. **2012**, *134* (18), 7632–7635.

(31) He, J.; Zhang, P.; Babu, T.; Liu, Y.; Gong, J.; Nie, Z. Near-Infrared Light-Responsive Vesicles of Au Nanoflowers. *Chem. Commun.* **2013**, *49* (6), 576–578.

(32) Song, J.; Zhou, J.; Duan, H. Self-Assembled Plasmonic Vesicles of SERS-Encoded Amphiphilic Gold Nanoparticles for Cancer Cell Targeting and Traceable Intracellular Drug Delivery. *J. Am. Chem. Soc.* **2012**, *134* (32), 13458–13469.

(33) Niikura, K.; Iyo, N.; Matsuo, Y.; Mitomo, H.; Ijiro, K. Sub-100 Nm Gold Nanoparticle Vesicles as a Drug Delivery Carrier Enabling Rapid Drug Release upon Light Irradiation. *ACS Appl. Mater. Interfaces* **2013**, *5* (9), 3900–3907.

(34) Velleman, L.; Scarabelli, L.; Sikdar, D.; Kornyshev, A. A.; Liz-Marzán, L. M.; Edel, J. B. Monitoring Plasmon Coupling and SERS Enhancement through: In Situ Nanoparticle Spacing Modulation. *Faraday Discuss.* **2017**, *205*, 67–83.

(35) Jain, P. K.; El-Sayed, M. A. Plasmonic Coupling in Noble Metal Nanostructures. *Chem. Phys. Lett.* **2010**, *487* (4–6), 153–164.

(36) Yahara, T.; Koga, T.; Yoshida, S.; Nakagawa, S.; Deguchi, H.; Shirouzo, K. Relationship between Microvessel Density and Thermographic Hot Areas in Breast Cancer. *Surg. Today* **2003**, *33* (4), 243–248.

(37) Otsuka, H.; Nagasaki, Y.; Kataoka, K. PEGylated Nanoparticles for Biological and Pharmaceutical Applications. *Adv. Drug Deliv. Rev.* **2003**, *55* (3), 403–419.

(38) Duncan, R. THE DAWNING ERA OF POLYMER THERAPEUTICS. *Nat. Rev. Drug Discov.* **2003**, *2*, 347–360.

(39) Kolate, A.; Baradia, D.; Patil, S.; Vhora, I.; Kore, G.; Misra, A. PEG - A Versatile Conjugating Ligand for Drugs and Drug Delivery Systems. *J. Control. Release* **2014**, *192*, 67–81.

(40) Poudel, A. J.; He, F.; Huang, L.; Xiao, L.; Yang, G. Supramolecular Hydrogels Based on Poly (Ethylene Glycol)-Poly (Lactic Acid) Block Copolymer Micelles and α-Cyclodextrin for Potential Injectable Drug Delivery System. *Carbohydr. Polym.* **2018**, *194* (April), 69–79.

(41) Tomczyk, E.; Promiński, A.; Bagiński, M.; Górecka, E.; Wójcik, M. Gold Nanoparticles Thin Films with Thermo- and Photoresponsive Plasmonic Properties Realized with Liquid-Crystalline Ligands. *Small* **2019**, *15* (37), 1–8.

(42) Housni, A.; Zhao, Y. Gold Nanoparticles Functionalized with Block Copolymers Displaying Either LCST or UCST Thermosensitivity in Aqueous Solution. *Langmuir* **2010**, *26* (15), 12933–12939.

(43) Liu, G.; Wang, D.; Zhou, F.; Liu, W. Electrostatic Self-Assembly of Au Nanoparticles onto Thermosensitive Magnetic Core-Shell Microgels for Thermally Tunable and Magnetically Recyclable Catalysis. *Small* **2015**, *11* (23), 2807–2816.

(44) Liu, Y.; Han, X.; He, L.; Yin, Y. Thermoresponsive Assembly of Charged Gold Nanoparticles and Their Reversible Tuning of Plasmon Coupling. *Angew. Chemie - Int. Ed.* **2012**, *51* (26), 6373–6377.

(45) Zhu, M. Q.; Wang, L. Q.; Exarhos, G. J.; Li, A. D. Q. Thermosensitive Gold Nanoparticles. *J. Am. Chem. Soc.* **2004**, *126* (9), 2656–2657.

(46) Zámbó, D.; Radnóczi, G. Z.; Deák, A. Preparation of Compact Nanoparticle Clusters from Polyethylene Glycol-Coated Gold Nanoparticles by Fine-Tuning Colloidal Interactions. *Langmuir* **2015**, *31* (9), 2662–2668.

(47) Boyer, C.; Whittaker, M. R.; Luzon, M.; Davis, T. P. Design and Synthesis of Dual Thermoresponsive and Antifouling Hybrid Polymer/Gold Nanoparticles. *Macromolecules* **2009**, *42* (18), 6917–6926.

(48) Shan, J.; Zhao, Y.; Granqvist, N.; Tenhu, H. Thermoresponsive Properties of N-Isopropylacrylamide Oligomer Brushes Grafted to Gold Nanoparticles: Effects of Molar Mass and Gold Core Size. *Macromolecules* **2009**, *42* (7), 2696–2701.

(49) Jones, S. T.; Walsh-Korb, Z.; Barrow, S. J.; Henderson, S. L.; Del Barrio, J.; Scherman, O. A. The Importance of Excess Poly(N-Isopropylacrylamide) for the Aggregation of Poly(N-Isopropylacrylamide)-Coated Gold Nanoparticles. *ACS Nano* **2016**, *10* (3), 3158–3165.

(50) Kotal, A.; Mandal, T. K.; Walt, D. R. Synthesis of Gold-Poly(Methyl Methacrylate) Core-Shell Nanoparticles by Surface-Confined Atom Transfer Radical Polymerization at Elevated Temperature. *J. Polym. Sci. Part A Polym. Chem.* **2005**, *43* (16), 3631–3642.

(51) Kurzhals, S.; Zirbs, R.; Reimhult, E. Synthesis and Magneto-Thermal Actuation of Iron Oxide Core-PNIPAM Shell Nanoparticles. *ACS Appl. Mater. Interfaces* **2015**, *7* (34), 19342–19352.

(52) Chakraborty, S.; Bishnoi, S. W.; Pérez-Luna, V. H. Gold Nanoparticles with Poly(N -Isopropylacrylamide) Formed via Surface Initiated Atom Transfer Free Radical Polymerization Exhibit Unusually Slow Aggregation Kinetics. *J. Phys. Chem. C* **2010**, *114* (13), 5947–5955.

(53) Dahl, J. A.; Maddux, B. L. S.; Hutchison, J. E. Toward Greener Nanosynthesis. *Chem. Rev.* **2007**, *107* (6), 2228–2269.

(54) Nuzzo, R. G.; Zegarski, B. R.; DuBois, L. H. Fundamental Studies of the Chemisorption of Organosulfur Compounds on Au(111). Implications for Molecular Self-Assembly on Gold Surfaces. *J. Am. Chem. Soc.* **1987**, *109* (3), 733–740.

(55) Love, J. C.; Estroff, L. A.; Kriebel, J. K.; Nuzzo, R. G.; Whitesides, G. M. *Self-Assembled Monolayers of Thiolates on Metals as a Form of Nanotechnology*; 2005; Vol. 105.

(56) Sethuraman, A.; Han, M.; Kane, R. S.; Belfort, G. Effect of Surface Wettability on the Adhesion of Proteins. *Langmuir* **2004**, *20* (18), 7779–7788.

(57) Iida, R.; Mitomo, H.; Niikura, K.; Matsuo, Y.; Ijiro, K. Two-Step Assembly of Thermoresponsive Gold Nanorods Coated with a Single Kind of Ligand. *Small* **2018**, *14* (14), 1–8.

(58) Iida, R.; Mitomo, H.; Matsuo, Y.; Niikura, K.; Ijiro, K. Thermoresponsive Assembly of Gold Nanoparticles Coated with Oligo(Ethylene Glycol) Ligands with an Alkyl Head. *J. Phys. Chem. C* **2016**, *120* (29), 15846–15854.

(59) Liu, X.; Li, H.; Jin, Q.; Ji, J. Surface Tailoring of Nanoparticles via Mixed-Charge Monolayers and Their Biomedical Applications. *Small* **2014**, *10* (21), 4230–4242.

(60) Eshhar, Z.; Reiter, Y.; Sivan, U. Controlled Platform for Studying Cell − Ligand Interactions. *Nano Lett.* **2012**, *12*, 4992.

(61) Ghorai, P. K.; Glotzer, S. C. Atomistic Simulation Study of Striped Phase Separation in Mixed-Ligand Self-Assembled Monolayer Coated Nanoparticles. *J. Phys. Chem. C* **2010**, *114* (45), 19182–19187.

(62) Petrie, T. A.; Stanley, B. T.; García, A. J. Micropatterned Surfaces with Controlled Ligand Tethering. *J. Biomed. Mater. Res. A* **2009**, *90* (3), 755–765.

Chapter 2

Precise Control of Thermo-responsiveness of AuNPs

by Surface Modification with Mixed Ligand

Abstract:

Thermo-responsive assembly of gold nanoparticles selectively occurring in body temperature of tumor tissues is a promising method to tumor-targeted photothermal cancer therapy as NIR absorption on assemblies. Our group have prepared OEG-alkanethiol modified AuNPs show the controllable thermo-responsiveness. For bio-application, precise control of thermo-responsiveness is required. Herein, I reported precise tuning of thermo-responsive properties of gold nanoparticles by surface modification with mixed OEG-attached alkanethiols. Importantly, the assembly temperature of OEG-alkanethiols modified AuNPs depend on both the hydrophobicity at the terminus and the core size of nanoparticles. Therefore, firstly, I precisely tune the terminal hydrophobicity by mixing two kinds of thermo-responsive OEG-alkanethiol with different hydrophobic terminus. Further, since precise core size control is difficult, I used a non-thermo-responsive ligand with a shorter OEG length to tune the local OEG density to reach the core size effect. Although the changes in local environment and configuration of ligands on dynamics remain unclear, experiment results support precise control of thermo-responsiveness by tuning of terminal hydrophobicity and local OEG density of alkanethiol ligands on surface.

KEYWORDS: oligo (ethylene glycol), thermo-responsiveness, gold nanoparticles, mixed ligands, precise control

2.1. Introduction

Molecules expand their functionalities as polymers and/or supra-molecules through connecting, concatenating, or assembling them. For example, in nature, enzymes, which are proteins produced by self-organization of amino acids and exhibit high catalytic activities which are not found in amino acids as monomers.[1–3] On the other hand, the control of assembly of chemical components support the creation of new materials which show functions close to even beyond natural ones.[4–6]

OEG and PEG, produced by self- organization of ethylene glycol, are one of the most important synthetic molecules for medical and therapeutic applications due to their properties, such as neutral charge, water-solubility, and biocompatibility.[7–11] PEG/OEG possesses not only bio-compatibility properties but also thermo-responsiveness on hydration/dehydration states.[12] On the other hand, OEG-derivative-grafted polymers[13,14] and OEG-derivative-attached detergent assemblies (micelles)[15,16] also show thermo-responsiveness as hydration/dehydration phenomena at lower critical solution temperature (LCST). Further, the copolymerization of two OEG macromonomers of different chain-lengths with different hydrophilicity leads to the formation of thermosensitive copolymers with a tunable LCST).[17,18] These kinds of thermo-responsive polymers with tunable LCST are now under the spotlight for therapeutic applications.[19]

Recently, gold nanoparticles (AuNPs) have attract much attention for therapeutic applications due to their plasmonic properties.[20–22] However, when using AuNPs, surface modification remains an issue for the provision of stable dispersibility in solution.. To this end, hydrophilic biocompatible polymers, such as PEG or OEG, are attached to their surfaces. Here, in terms of the surface modification of nanoparticles, there is one unmistakable fact: nanoparticle curvature controls the molecular conformation and

chemical properties of the attached molecules by changing their local density or distances (in a range between 4–20 nm of AuNP diameter).[23–25]

Our group previously reported that AuNPs covered with OEG-attached alkanethiols show thermo-responsive assembly caused by hydrophobic interactions from dehydration of OEG portions.[26] Importantly, their thermo-responsiveness significantly depends on the hydrophobic terminus of alkanethiols like 56, 26, and 19 °C of terminus as ethyl, isopropyl, and propyl, respectively. For bio-application, precise control of thermo-responsiveness is required. On the other hand, Iida et al. demonstrated the hierarchical self-assembly of rod-shaped gold nanoparticles based on curvature-dependent thermoresponsiveness.[27] It seems useful that nanoparticle size-based tuning of T_A, as it shows drastic changes like 67, 56, and 39 °C in 3, 5, and 10 nm in diameter, respectively.[26] However, as the exact control in NP sizes or curvature remains difficult, they could not precisely tune their T_A, missing potential applications. According to the copolymers with a tunable LCST and core size dependent local OEG density, surface modification with mixed ligands is supposed to be effective to tuning of terminal hydrophobicity and local OEG density to reach the core size effect. Therefore, in this study, I report a novel T_A tuning approach for AuNPs coated with OEG-derivatives by the hydrophobic terminus and local OEG density control of thermo-responsive OEG-derivatives (C2-EG6-C11-SH) via mixing with another thermo-responsive OEG-derivatives (C1-EG6-C11-SH) and non-thermo-responsive short ligands (HO-EG2-C11-SH) (Scheme 2-1).

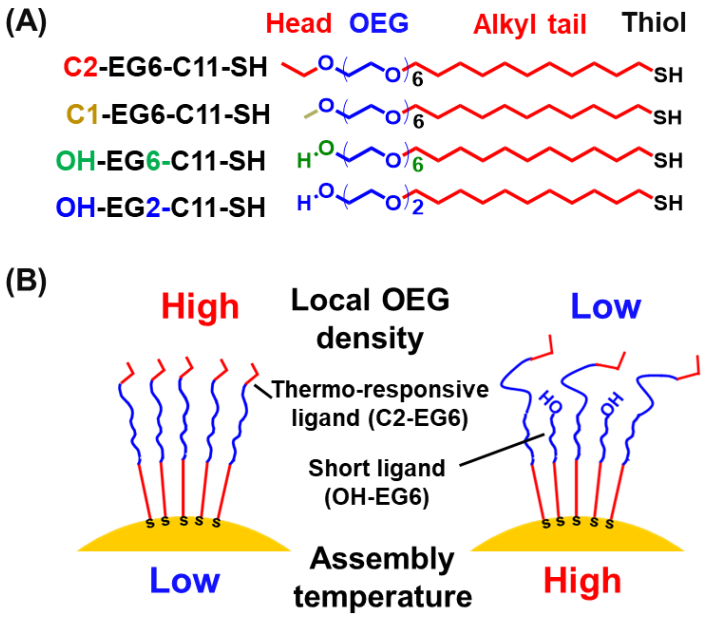

Scheme 2-1. (A) Chemical structures of the surface ligands used in this study and (B) an illustration of surface ligands attached on the AuNPs.

2-2. Experimental section

2-2-1 Materials and instruments

Citrate-protected AuNPs in aqueous solution (10, 15, and 20 nm in diameter) were purchased from BBI Solutions (UK). Surface ligands with a methyl, ethyl, and hydroxyl head, referred to as C1-EG6-C11-SH, C2-EG6-C11-SH, HO-EG6-C11-SH, and HO-EG2-C11-SH, respectively, were synthesized according to our previous paper (Scheme 2).[28,29] The other solvents were purchased from Wako Pure Chemical Industries Ltd. (Japan). All commercially available reagents were used without further purification. Thin-layer chromatography (TLC) was performed on glass-backed precoated silica gel plates (60F254, Merck & Co., Inc., USA). Cerium molybdate (10% Cerium (IV) Sulphate, 15%H2SO4 aqueous solution) was used as a coloring agent. Organic solvents were evaporated with an evaporator (TOKYO RIKAKIKAI Co., Ltd). Products were isolated by column chromatography on silica-gel (Kanto Chemical, neutral 60N, 40−50 μm). NMR spectra were recorded on a 400 MHz JEOL spectrometer. High-resolution ESI-MS spectra were measured with an Exactive LCMS Mass Spectrometer (Thermo Fisher Scientific Inc., Japan) by the Instrumental Analysis Division, Equipment Management Center Creative Research Institution, Hokkaido University. AuNPs were analyzed by UV-Vis/NIR spectrophotometer (V-770, JASCO corp.) and dynamic light scatting (DLS) (Zetasizer Nano ZS, Malvern Panalytical).

2-2-2 Synthesis of HO-EG2-C11-SH

Scheme 2-2. Chemical synthesis of **HO-EG2-C11-SH** ligands

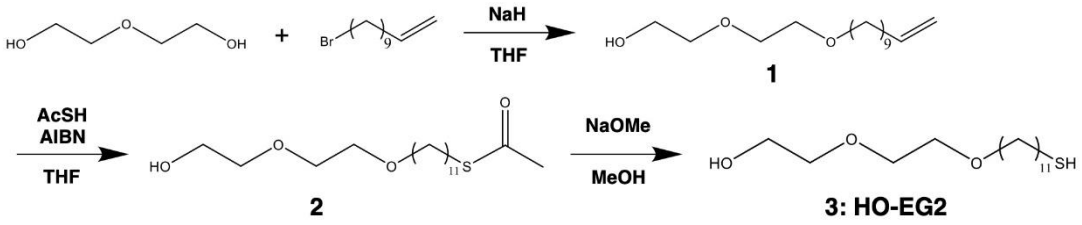

Synthesis of 3,6-Dioxa-16-heptadecen-1-ol; (1)

Diethylene glycol (14.9g, 140 mmol) was dissolved in THF (55 ml). The solution was cooled on ice and added sodium hydride (60% in oil, 4.26 g, 106.4 mmol) and 11-bromo-1-undecene (6.53 ml, 28 mmol). The mixture was stirred at room temperature for 16 h, and then refluxed at 80°C for 16 h. After removal of the solvent, the residue was dissolved in solution (EtOAc/Hexane (1:1), 200 ml) and washed twice with a saturated NaCl solution. The organic layer was dried over anhydrous Na_2SO_4. The crude product was concentrated in vacuo and purified by flash chromatography on silica gel (Hexane/EtOAc (2:1)) to yield compound **1** (1.85g, 25%).

^{1}H NMR (400 MHz, $CDCl_3$): δ /ppm = 1.25-1.32 (m, 12H, alkyl chain), 1.56-1.60 (m, 2H, alkyl chain), 1.98-2.03 (q, 2H, -CH_2-*CH_2*-CH=), 2.48 (s, 1H, *HO*-), 3.42-3.72 (m, 10H, -*CH_2*-O-), 4.88-4.99 (m, 2H, -CH=*CH_2*), 5.74-5.84 (m, 1H, -*CH*=CH_2).

Synthesis of Ethanethioic acid, S-[11-[2-(2-hydroxyethoxy) ethoxy] undecyl] ester; (2)

Compound **1** (1.00 g, 3.87 mmol), thioacetic acid (1.52 g, 20.0 mmol), and 2,2'-azobisisobutyronitrile (0.636 g, 3.87 mmol) were dissolved in stabilizer free dry THF (30 mL). The mixture was stirred for 3 h at 80 °C under N_2 atmosphere. The mixture was

evaporated under vacuum. The crude product was concentrated in vacuo and purified by flash chromatography on silica gel (Hexane/EtOAc (1:1)) to yield compound **2** (0.65 g, 50 %) as a clear syrup.

^{1}H NMR (400 MHz, $CDCl_3$): δ /ppm = 1.26-1.32 (m, 14H, alkyl chain), 1.57-1.60 (m, 4H, alkyl chain), 2.30-2.32 (s, 3H, -S-CO-*CH_3*), 2.84-2.87 (t, 2H, -CH_2-*CH_2*-S-), 3.44-3.49 (t, 2H, HO-*CH_2*-), 3.58-3.73 (m, 8H, -*CH_2*-O-).

Synthesis of 2-[2-[(11-Mercaptoundecyl) oxy] ethoxy] ethanol; (3) HO-EG2-C11-SH

Compound **2** (0.65 g, 1.94 mmol) and sodium methoxide (powder, 0.52g, 9.7 mmol) were dissolved in 20 mL MeOH, and the mixture was stirred over night at 30 °C. After adding HCl aq. until the solution pH<7, the solvent was removed under vacuum. The residue was dissolved in EtOAc and washed twice with sat. NaCl solution. The organic layer was dried over anhydrous Na_2SO_4. The crude product was concentrated in vacuo and purified by flash chromatography on silica gel (Hexane/Acetone (2:3)) to yield compound **3** (0.07g 12.5%) as a clear syrup.

^{1}H NMR (400 MHz, $CDCl_3$): δ /ppm = 1.26-1.38 (m, 14H, alkyl chain), 1.55-1.62 (m, 4H, alkyl chain), 2.49-2.54 (q, 2H, -*CH_2*-SH), 3.44-3.48 (t, 2H, HO-*CH_2*-), 3.57-3.73 (m, 8H, -*CH_2*-O-).

HR-MS (ESI): calcd for $C_{15}H_{32}O_3SNa$ $[M+Na]^+$ 315.19644, found 315.19615.

2-2-3. Surface modification of AuNPs

AuNPs coated with oligo (ethylene glycol) derivatives were prepared via a ligand exchange reaction. Briefly, 1 mL of citrate-coated AuNPs (10, 15, and 20 nm) were concentrated by centrifugation (12,000 g for 45 min) and the following removal of the

supernatant (900 μL). The concentrated citrate-protected 10 nm-AuNPs (94 μM, 100 μL), 15 nm-AuNPs (23 μM, 100 μL), and 20 nm-AuNPs (12 μM, 100 μL) were mixed with the thiolate ligand molecules including tris (2-carboxyethl) phosphine (TCEP) as a reductant. In this exchange reaction, the total ligand concentration was adjusted to 10 equivalents for the surface atoms on a AuNP.[30] In the case of 10 nm AuNPs, the number of surface Au atoms was 4192/particle and the concentration of the ligand solution was 4.0 mM. In the case of 15 nm and 20 nm AuNPs, the number of surface Au atoms was 9585 and 17178/particle, respectively, and both of the ligand concentration was 2.0 mM. After the addition of ultrapure water up to 500 μL, the AuNPs were incubated for 48 h at 4 °C. Then, the surface modified AuNPs were washed 3 times by centrifugation (12,000 g for 45 min), the removal of the supernatant (470 μL), and addition of 10 mM HEPES buffer (pH 8.0) up to 500 μL to remove the free thiol ligands.

2-2-4. UV–vis–NIR spectroscopy

The UV–vis–NIR spectra of the AuNPs were measured using a V-770 UV-Visible/NIR Spectrophotometer with PAC-743R automatic 6 position Peltier cell changer (JASCO corp, Japan). The temperature-change measurements of the AuNP spectra were performed at each temperature changed by the rate of 1°C/min followed by 5 min waiting time.

2-2-5. Dynamic light scattering (DLS) and zeta-potential measurement

The size and zeta-potential of AuNPs were measured using a Zetasizer Nano ZS (Malvern Panalytical Ltd, UK). The temperature-change measurements of the AuNPs sizes were performed at each temperature after 2 min-waiting time. The assembly

temperature was defined as the middle temperature between the temperature at which the size of AuNPs shows a significant change and the highest temperature for AuNPs remaining dispersed.

2-3. Results and discussion

2-3-1. Thermo-responsive properties of AuNPs coated with C1- or C2-EG6-C11-SH ligands

First, I prepared thermo-responsive AuNPs by surface modification with a C1- or C2-EG6-C11-SH ligand. The AuNP (diameter of 10, 15, and 20 nm) surfaces were modified with alkane thiol ligands via replacing with citrate in water according to Iida et al.'s paper.[26] Citric acid and excess ligands were removed, and their solvent was replaced to 10 mM HEPES buffer (pH 8.0) via repetitive centrifugal purifications. Results for dynamic light scattering (DLS), zeta-potential, and extinction spectral analyses support successful surface modifications (Table 2-1 and Figure 2-1). Briefly, DLS measurements showed an increase of several nm in hydrodynamic diameters of AuNPs by the surface modification with OEG-derivatives. The zeta-potential of the AuNPs changed from negative (*ca*. -30 mV in citric acid solution) for the citrate-protected AuNPs to weak negative (-8.7 ± 4.9 and -10.6 ± 3.1 mV in buffer) for C1- and C2-EG6-C11-SH-coated AuNPs (*d*=15 nm), respectively. Extinction spectra show a slight red-shift of plasmonic absorption peak from 517, 520, and 532 nm for citrate-coated to 522, 523, and 532 nm for C2-EG6-C11-SH-coated of AuNPs (10, 15, 20 nm), respectively, due to the refractive index changes around AuNPs.

The thermo-responsiveness was then investigated by spectral and DLS analyses. Spectral changes indicate that C2-EG6-C11-SH-coated AuNPs (15 nm) showed thermo-responsive assembly between 30 and 35 °C (Figure 2-2A). Importantly, DLS measurements show clear changes in size distribution responding to temperature changes in the heating and cooling processes (Figure 2-2B). In the case of C2-EG6-C11-SH-coated AuNPs (15 nm), assembly/disassembly transition was observed between 32 and

33°C. The assembly temperature of this experiment was, therefore, regarded as 32.5 ℃. The temperature for their thermo-responsive assembly (T_A) was determined as 32.5 ± 1.0 °C from three independent DLS analyses on heating. Similarly, T_A of C2-EG6-C11-SH-coated AuNPs of different diameter (10 nm and 20 nm) were determined to be 43.5 ± 3.5 °C and 24.2 ± 1.5 °C, respectively (Table 2-2 and Figure 2-3 and 4 blue). The T_A values of C1-EG6-C11-SH-coated AuNPs were also determined (Table 2-2 and Figure 2-4 red). Figure 2-4 clearly shows the C2-EG6-C11-SH ligand provided a lower T_A compared to the C1-EG6-C11-SH ligand due to the hydrophobicity at its terminus, while the higher curvature from the smaller particle size provided a higher T_A, findings which correspond to those reported by Iida *et al.*[26]

Table 2-1. Hydrodynamic diameter and zeta-potential of AuNPs before and after surface modifications with a **C1-** or **C2-EG6-C11-SH** ligand.

10 nm AuNP	Zeta-Potential (mV)	S.D.	Size*[1] (nm)	S.D.
Citric Acid	-26.9	2.5	10.4	0.2
C1 100%	-7.5	2.1	13.6	0.6
C2 100%	-8.0	0.5	13.7	0.6
15 nm AuNP	Zeta-Potential (mV)	S.D.	Size*[1] (nm)	S.D.
Citric Acid	-31.3	1.4	15.1	0.6
C1 100%	-8.7	4.9	22.6	6.3
C2 100%	-10.6	3.1	19.7	0.3
20 nm AuNP	Zeta-Potential (mV)	S.D.	Size*[1] (nm)	S.D.
Citric Acid	-37.7	2.5	19.2	0.2
C1 100%	-9.0	1.9	50.5	50.3
C2 100%	-14.3	0.6	26.7	4.0

*[1] Size was determined as a main peak size in DLS size distribution by volume. Large size AuNPs (20 nm) could result from a partial aggregation due to their hydrophobicity.

Table 2-2. Assembly temperature of AuNPs of different diameter (10 nm, 15 nm and 20 nm) modified with mixed ligands: (A) C2-EG6-C11-SH; (B) C1-EG-6C11-SH.

(**A**)

C2-EG6-C11-SH	Assembly *1 Temperature (ºC)	S. D.
10 nm AuNPs@	43.5	3.5
15 nm AuNPs@	32.5	1
20 nm AuNPs@	24.2	1.5

(**B**)

C1-EG6-C11-SH	Assembly *1 Temperature (ºC)	S. D.
10 nm AuNPs@	72.8	4.7
15 nm AuNPs@	63.2	2.5
20 nm AuNPs@	52.8	2.9

*1 T_A was from three independent DLS analysis.

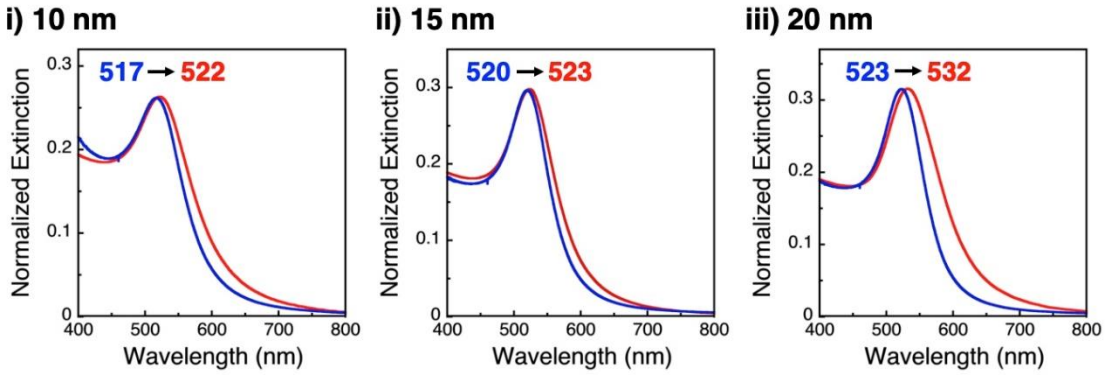

Figure 2-1. Extinction spectra of AuNPs with 10 nm (i), 15 nm (ii), and 20 nm in a diameter (iii) before (blue) and after surface modification with **C2-EG6** ligands (red). The numbers indicate their peak wavelength.

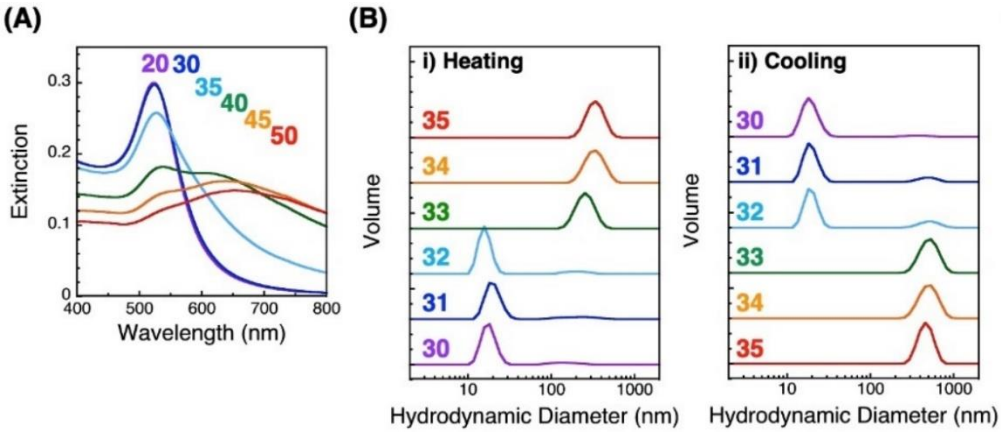

Figure 2-2. Thermo-responsive phenomena of AuNPs coated with **C2-EG6-C11-SH** ligands. (A) Extinction spectra of **C2-EG6-C11-SH** -coated AuNPs (15 nm) on a heating process. (B) Size distribution of **C2-EG6-C11-SH** -coated AuNPs (15 nm) measured by DLS. Colored numbers in (A) and (B) mean solution temperature.

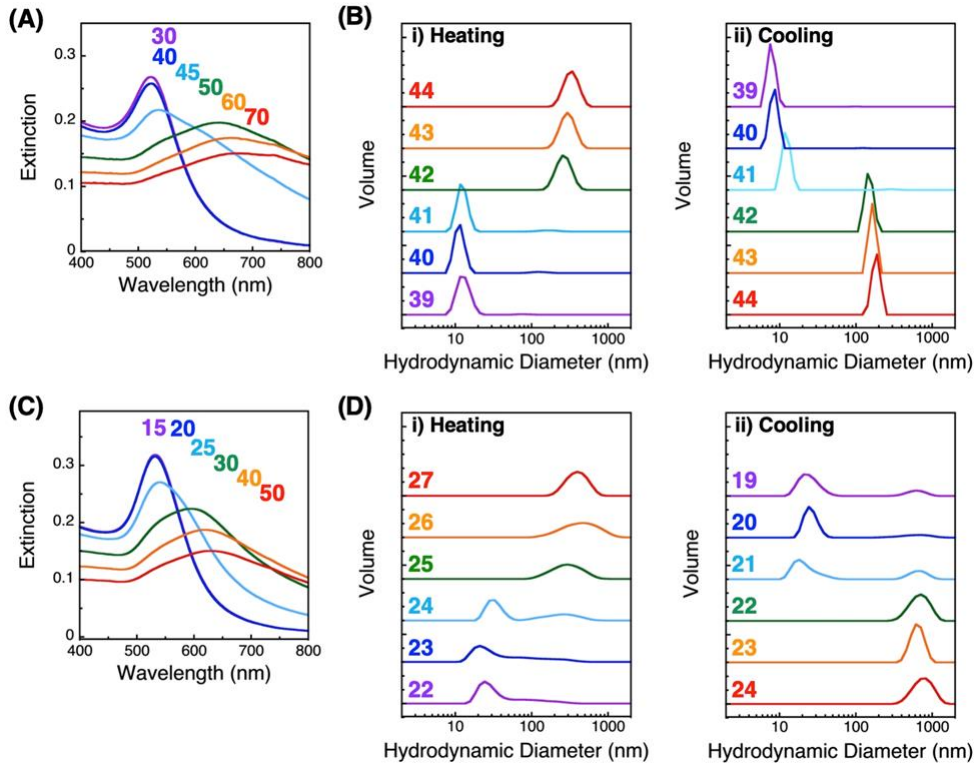

Figure 2-3. Thermo-responsive phenomena of AuNPs coated with **C2-EG6-C11-SH** ligands: Extinction spectra (A)(C) and size distribution (B)(D) of C2-EG6 ligand-modified AuNPs which have 10 nm (A)(B) and 20 nm in a diameter (C)(D).

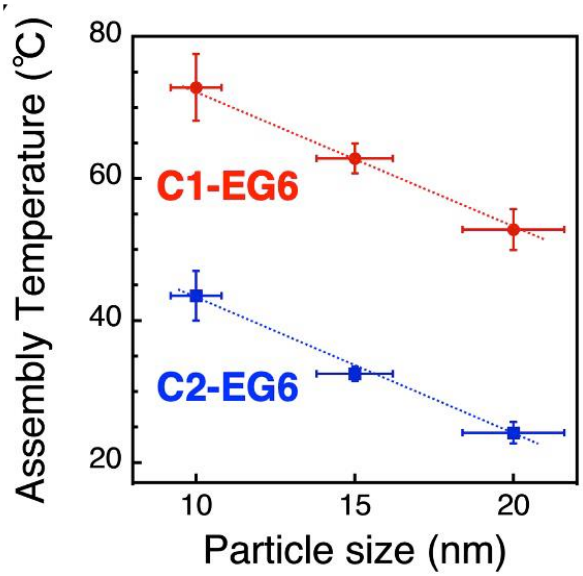

Figure 2-4. Assembly temperatures of 10, 15, and 20 nm AuNPs coated with **C1-EG6** (red) and **C2-EG6** ligands (blue). Error bars in y-axis represent a standard deviation determined from three independent experiments. Error bars in x-axis represent a coefficient of variation determined by BBI solutions. Dotted lines are shown as a guide.

2.3-2. Tuning of assembly temperature by hydrophobicity control via mixing of X-EG6 ligands

Precise tuning of the assembly temperature is an important issue for bio-related applications, particular turning around 37 °C. Fig. 2-4 shows 2 °C decrease in T_A with a 1 nm size increase in diameter, suggesting that extreme control of AuNP size or shape can provide precise tunability. Although preparation techniques for nanoparticles have greatly advanced recently, size control on a sub-nm scale remains quite difficult.[31] For example, BBI solutions provides AuNPs of well-controlled sizes, which we used in this study, with a variation coefficient of within 8%. That is *ca*. 1 nm size distribution for 15 nm AuNPs, resulting in a 2 °C variation in T_A. Thus, we performed assembly temperature tuning using ligand mixing as another approach using 15 nm AuNPs. First, I focused on the tuning of hydrophobicity by mixing surface ligands with different termini. For the surface modification of 15 nm AuNPs, I applied thermo-responsive ligands of **C1-EG6-C11-SH** and **C2-EG6-C11-SH** at various mixing ratios. These AuNPs showed obvious shifts in assembly temperature between 33 °C for 100% **C2-EG6-C11-SH** and 63 °C for 100% **C1-EG6-C11-SH** (Table 2-3A and Figure 2-5 red). As it is well-known that the LCST of thermo-responsive polymers, such as pNIPAm, is shifted to a lower temperatures by the addition of hydrophobic moieties,[32] this result is as expected. On the other hand, a great increase in assembly temperature observed on by mixing with a **HO-EG6-C11-SH** ligand, which has neutral hydrophilic terminus, was impressive (Table 2-3B and Figure 2-5 blue). In any case, it is possible to tune the assembly temperature by controlling the hydrophobicity at the terminus. Interestingly, the shape of C1-EG6-C11-SH/C2-EG6-C11-SH curves showed an obvious convex, whereas the standard linear relationship, and the real T_A is slightly higher than the theoretical value, suggesting the

bias modification existed, which C1-EG6-C11-SH attached to AuNPs much more than C21-EG6-C11-SH. Until now, control of surface modification proceeding as the additional ratios of mixed ligands remain an issue. Importantly, even though there is a little bias modification, as the ligand mixing ratio is easily and precisely tunable, this is an effective approach.

Table 2-3. Assembly temperature of AuNPs (15 nm) modified with mixed ligands: (A) C1-EG6-C11-SH and C2-EG6-C11-SH; (B) OH-EG-6C11-SH and C2-EG-6C11-SH.

(**A**)

C2-EG6 : C1-EG6 Ligand Ratio	Assembly *1 Temperature (ºC)	S. D.
95 : 5	37.8	2.5
90 : 10	41.8	1.5
75 : 25	47.5	2.6
50 : 50	53.2	2.3
25 : 75	59.2	1.2
5 : 95	62.5	2.6

(**B**)

C2-EG6 : OH-EG6 Ligand Ratio	Assembly *1 Temperature (ºC)	S. D.
95 : 5	51.8	2.9
90 : 10	63.8	2.9

*1 T_A was from three independent DLS analysis.

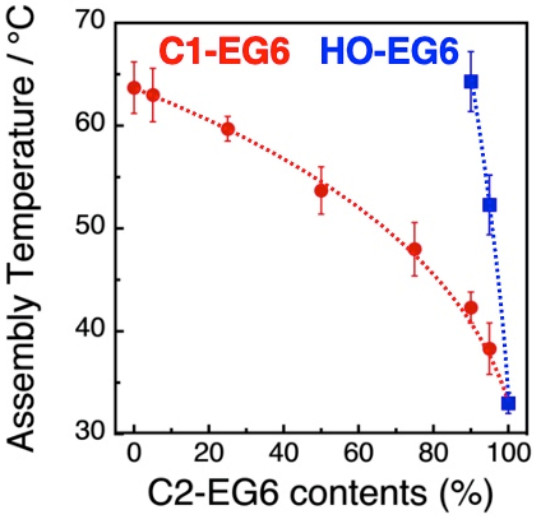

Figure 2-5. Assembly temperatures of 15 nm-sized AuNPs coated with a mixture of **C1-** and **C2-EG6-C11-SH** ligands (red) and **C2-** and **HO-EG6-C11-SH** ligands (blue). Dotted lines are shown as a guide.

2-3-3. Tuning of assembly temperature by local OEG density control via mixing of OEG derivatives with a different OEG length

Next, I focused on the effect of surface curvature (nanoparticle size) on the control their thermo-responsive assembly. It has been reported that the surface ligand density on AuNPs was determined to be *ca.* 5 molecules/nm^2 by inductively coupled plasma atomic emission spectroscopy (ICP-AES) and was independent of their size and shapes.[26,27] Surface curvature induces a different local density of the OEG portion at the outer surface, although their molecular density at the AuNP surface remain the same. Thus, I hypothesized their local density, which is related to the molecular free volume, is one of the key factors in tuning their assembly temperature. To tune their local density, here, we mixed the thermo-responsive ligand, C2-EG6-C11-SH, with a non-thermo-responsive ligand with a shorter OEG chain-length, HO-EG2-C11-SH (Scheme 2-1).

Assembly temperatures of 15 nm AuNPs coated with a mixture of C2-EG6-C11-SH and HO-EG2-C11-SH ligands was investigated in the same manner as described above (Table 2-4). The plots of T_A by the ligand mixing ratios of C2-EG6-C11-SH to HO-EG2-C11-SH clearly indicates that the local molecular density tuned by mixing with a short-chain OEG ligand a significantly linear effect on T_A (Figure 2-6). This increase in T_A by the replacement of C2-EG6-C11-SH with HO-EG2-C11-SH also include changes in the hydrophobicity at the terminus. To discuss the effects of the tuning of local molecular density by mixing with a short-chain OEG ligand, comparisons of these ligand replacements by C1-EG6-C11-SH, HO-EG6-C11-SH, and HO-EG2-C11-SH are important. As the hydrophobic effect from the HO-EG2-C11-SH portion is expected to be lower than that from C1-EG6-C11-SH portion and similar to the HO-EG6-C11-SH portion, this more moderate linear about C2-EG6-C11-SH /HO-EG2-C11-SH increase in

T_A (Figure 2-6), which is compared to C2-EG6-C11-SH / HO-EG6-C11-SH (Figure 2-4), can be concluded to be mainly result from the tuning of local molecular density. Also, the difference in the correlation curves between the linear curve for C2-EG6/HO-EG2 (Fig. 2-6) and the convex curve for C2-EG6/C1-EG6 or HO-EG6 (Fig. 2-5) implies variations in their origin.

In these experimental results, the **C2-EG6-C11-SH** contents on the x-axis are shown as a ligand mixing ratio in the surface modification process as the real ligand content on the AuNP surfaces was unclear due to the experimental difficulties. Nevertheless, the convex shape curve of C1-EG6-C11-SH/ C2-EG6-C11-SH have simply showed the unfairness on surface modification. Next chapter, I will introduce the investigation on this unfairness.

Table 2-4. Assembly temperature of AuNPs modified with mixed ligands: C2-EG2-C11-SH and C2-EG6-C11-SH.

C2-EG6 : OH-EG2 Ligand Ratio	Assembly *1 Temperature (°C)	S. D.
80 : 20	36.5	2.0
60 : 40	40.5	3.6
40 : 60	43.5	4.4
20 : 80	48.2	3.8

*1 T_A was from three independent DLS analysis.

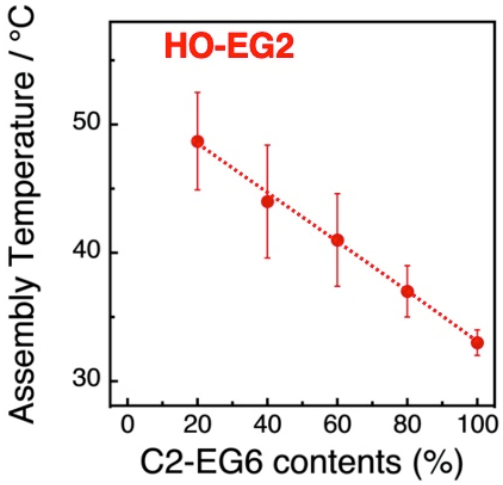

Figure 2-6. Assembly temperatures of 15 nm-sized AuNPs coated with a mixture of **C2-EG6** and **HO-EG2** ligands. Dotted line is shown as a guide.

2-4. Conclusion

In this study, thermo-responsive properties of oligo (ethylene glycol) (OEG) derivatives attached on the gold nanoparticles have been precisely tuned via the local environmental control not only by the hydrophobic moiety of their terminus but also by their local OEG density. OEG-attached alkane thiol-modified AuNPs showed thermo-responsive assembly/disassembly through the hydration/dehydration of OEG portions depending on the hydrophobicity at the terminus. Therefore, tuning of terminal hydrophobicity using mixed ligands of two kinds of alkanethiols with different hydrophobic terminus successfully tuned the thermo-responsiveness. Further, the core size of nanoparticles changes their responsive temperatures. The larger size provides the higher local OEG density, suggesting more packed adjacent OEG portions which are supposed to cause the increasing interaction of molecules and accelerate dehydration of themselves, resulting in lower assembly temperature. Importantly, the assembly temperature (T_A) was also tuned by the ligand mixing with a non-thermo-responsive ligand with a shorter OEG length to control the local density of OEG portion. Although the real motions of OEG portion remain unclear, experimental results on the core size dependence of T_A and the ligand mixing with a different OEG length support the local OEG density take effect. It is expected that precise control of thermo-responsiveness by surface modification with mixed ligands promote a simple way for bio-application such as photothermal tumor-targeted photothermal cancer therapy. Additionally, our finding in this study provides a novel molecular design to the tuning of their functionality based on the ligand properties and composition, leading to opening a door for novel emergent functions.

2-5. References

(1) Depeursinge, A.; Racoceanu, D.; Iavindrasana, J.; Cohen, G.; Platon, A.; Poletti, P.-A.; Muller, H. Fusing Visual and Clinical Information for Lung Tissue Classification in HRCT Data. *Artif. Intell. Med.* **2010**, *11* (Figure 1), ARTMED1118.

(2) Hammes-Schiffer, S.; Benkovic, S. J. Relating Protein Motion to Catalysis. *Annu. Rev. Biochem.* **2006**, *75*, 519–541.

(3) Warshel, A. Computer Simulations of Enzyme Catalysis: Methods, Progress, and Insights. *Annu. Rev. Biophys. Biomol. Struct.* **2003**, *32*, 425–443.

(4) Lehn, J. M. Perspectives in Chemistry - Steps towards Complex Matter. *Angew. Chemie - Int. Ed.* **2013**, *52* (10), 2836–2850.

(5) Lutolf, M. P.; Hubbell, J. A. Synthetic Biomaterials as Instructive Extracellular Microenvironments for Morphogenesis in Tissue Engineering. *Nat. Biotechnol.* **2005**, *23* (1), 47–55.

(6) Hawker, C. J.; Wooley, K. L. The Convergence of Synthetic Organic and Polymer Chemistries. *Science (80-.).* **2005**, *309* (5738), 1200–1205.

(7) Sigal, G. B.; Mrksich, M.; Whitesides, G. M. Effect of Surface Wettability on the Adsorption of Proteins and Detergents. *J. Am. Chem. Soc.* **1998**, *120* (14), 3464–3473.

(8) Kolate, A.; Baradia, D.; Patil, S.; Vhora, I.; Kore, G.; Misra, A. PEG - A Versatile Conjugating Ligand for Drugs and Drug Delivery Systems. *J. Control. Release* **2014**, *192*, 67–81.

(9) Otsuka, H.; Nagasaki, Y.; Kataoka, K. PEGylated Nanoparticles for Biological and Pharmaceutical Applications. *Adv. Drug Deliv. Rev.* **2003**, *55*, 403–419.

(10) Love, J. C.; Estroff, L. A.; Kriebel, J. K.; Nuzzo, R. G.; Whitesides, G. M. *Self-Assembled Monolayers of Thiolates on Metals as a Form of Nanotechnology*; 2005; Vol. 105.

(11) Duncan, R. THE DAWNING ERA OF POLYMER THERAPEUTICS. *Nat. Rev. Drug Discov.* **2003**, *2*, 347–360.

(12) Saeki, S.; Kuwahara, N.; Nakata, M.; Kaneko, M. Phase Separation of Poly (Ethylene Glycol) - Water-Salt Systems. *Polymer (Guildf).* **1977**, *18*, 1027–1031.

(13) Han, S.; Hagiwara, M.; Ishizone, T. Synthesis of Thermally Sensitive Water-Soluble Polymethacrylates by Living Anionic Polymerizations of Oligo(Ethylene Glycol) Methyl Ether Methacrylates. *Macromolecules* **2003**, *36*, 8312–8319.

(14) Skrabania, K.; Mertoglu, M.; Storsberg, J. Stimuli Responsive Amphiphilic Block Copolymers for Aqueous Media Synthesised via Reversible Addition Fragmentation Chain Transfer Polymerisation (RAFT). *Polymer (Guildf).* **2005**, *46*, 7726–7740.

(15) Schick M.J. Surface Films of Nonionic Detergents - I. Surface Tension Study. *J. Colloid Sci.* **1962**, *17*, 801–813.

(16) Tasaki, K. Poly(Oxyethylene)-Water Interactions : A Molecular Dynamics Study. *J. Am. Chem. Soc.* **1996**, *118*, 8459–8469.

(17) Lutz, J.-F.; Akdemir, Ö.; Hoth, A. Point by Point Comparison of Two Thermosensitive Polymers Exhibiting a Similar LCST: Is the Age of Poly(NIPAM) Over? *J. Am. Chem. Soc.* **2006**, *128* (40), 13046–13047.

(18) Lutz, J.-F.; Hoth, A. Preparation of Ideal PEG Analogues with a Tunable Thermosensitivity by Controlled Radical Copolymerization of 2-(2-Methoxyethoxy)Ethyl Methacrylate and Oligo(Ethylene Glycol) Methacrylate. *Macromolecules* **2006**, *39*, 893–896.

(19) Araki, T.; Murayama, S.; Usui, K.; Shimada, T.; Aoki, I.; Karasawa, S. Self-Assembly Behavior of Emissive Urea Benzene Derivatives Enables Heat-Induced Accumulation in Tumor Tissue. *Nano Lett.* **2017**, *17*, 2397–2403.

(20) Nambara, K.; Niikura, K.; Mitomo, H.; Ninomiya, T.; Takeuchi, C.; Wei, J.; Matsuo, Y.; Ijiro, K. Reverse Size Dependences of the Cellular Uptake of Triangular and Spherical Gold Nanoparticles. *Langmuir* **2016**, *32* (47).

(21) Dykman, L.; Khlebtsov, N. Gold Nanoparticles in Biomedical Applications: Recent Advances and Perspectives. *Chem. Soc. Rev.* **2012**, *41* (6), 2256.

(22) Tazaki, T.; Tabata, K.; Ainai, A.; Ohara, Y.; Kobayashi, S.; Ninomiya, T.; Orba, Y.; Mitomo, H.; Nakano, T.; Hasegawa, H.; et al. Shape-Dependent Adjuvanticity of Nanoparticle-Conjugated RNA Adjuvants for Intranasal Inactivated Influenza Vaccines. *RSC Adv.* **2018**, *8* (30).

(23) Walker, D. A.; Leitsch, E. K.; Nap, R. J.; Szleifer, I.; Grzybowski, B. A. Geometric Curvature Controls the Chemical Patchiness and Self-Assembly of Nanoparticles. *Nat. Nanotechnol.* **2013**, *8*, 676–683.

(24) Mandal, H. S.; Kraatz, H. Effect of the Surface Curvature on the Secondary Structure of Peptides Adsorbed on Nanoparticles. *J. Am. Chem. Soc.* **2007**, *129*, 6356–6357.

(25) Wang, D.; Nap, R. J.; Lagzi, I.; Kowalczyk, B.; Han, S.; Grzybowski, B. A.; Szleifer, I. How and Why Nanoparticle's Curvature Regulates the Apparent PKa of the Coating Ligands. *J. Am. Chem. Soc.* **2011**, *133* (7), 2192–2197.

(26) Iida, R.; Mitomo, H.; Matsuo, Y.; Niikura, K.; Ijiro, K. Thermoresponsive Assembly of Gold Nanoparticles Coated with Oligo(Ethylene Glycol) Ligands with an Alkyl Head. *J. Phys. Chem. C* **2016**, *120* (29), 15846–15854.

(27) Iida, R.; Mitomo, H.; Niikura, K.; Matsuo, Y.; Ijiro, K. Two-Step Assembly of Thermoresponsive Gold Nanorods Coated with a Single Kind of Ligand. *Small* **2018**, *14* (14).

(28) Iida, R.; Kawamura, H.; Niikura, K.; Kimura, T.; Sekiguchi, S.; Joti, Y.; Bessho, Y.; Mitomo, H.; Nishino, Y.; Ijiro, K. Synthesis of Janus-Like Gold Nanoparticles with Hydrophilic/Hydrophobic Faces by Surface Ligand Exchange and Their Self-Assemblies in Water. *Langmuir* **2015**, *31* (14), 4054–4062.

(29) Torii, Y.; Sugimura, N.; Mitomo, H.; Niikura, K.; Ijiro, K. PH-Responsive Coassembly of Oligo(Ethylene Glycol)-Coated Gold Nanoparticles with External Anionic Polymers via Hydrogen Bonding. *Langmuir* **2017**, *33* (22), 5537–5544.

(30) Oh, E.; Delehanty, J. B.; Sapsford, K. E.; Susumu, K.; Goswami, R.; Blanco-Canosa, J. B.; Dawson, P. E.; Granek, J.; Shoff, M.; Zhang, Q.; et al. Cellular Uptake and Fate of PEGylated Gold Nanoparticles Is Dependent on Both Cell-Penetration Peptides and Particle Size. *ACS Nano* **2011**, *5* (8), 6434–6448.

(31) Tsutsui, G.; Huang, S.; Sakaue, H.; Shingubara, S.; Takahagi, T. Well-Size-Controlled Colloidal Gold Nanoparticles Dispersed in Organic Solvents. *Japanese J. Appl. Physics, Part 1 Regul. Pap. Short Notes Rev. Pap.* **2001**, *40* (1), 346–349.

(32) Roy, D.; Brooks, W. L. A.; Sumerlin, B. S. New Directions in Thermoresponsive Polymers. *Chem. Soc. Rev.* **2013**, *42* (17), 7214–7243.

Chapter 3

Well-control of Ligand Exchange

for Fair Surface Modification

Abstract:

Control of composition of ligands on AuNP surface via modification with mixed ligand molecules at various ratio have been used for tuning of surface properties. Although these properties indeed changed by the control of mixing ligands ratio, it remains unclear whether surface modification proceeding as the mixing ratios. In chapter 2, biased surface modification was observed even though using the alkanethiols with similar structure. Ligand exchange between ligands attaching on surface and existing in solution is supposed to be one of the reasons of biased surface modification. Herein, I have confirmed that immobilized ligand in highly packed self-assembled monolayers (SAMs) are still replaced with the external ligands by ligand exchange through comparation of the assembly temperature (T_A) before and after addition of free ligand. I performed kinetic analyses by time course experiments and found the ligand exchange almost proceed as the ratio of ligands in the reaction medium firstly and then showed the unfairness on ligand exchange over time. Then I confirmed this unfair ligand exchange and determined the good surface modification conditions. Finally, based on investigation ligand exchange, I preformed the surface modification carefully and tried to approach to the fairness.

KEYWORDS: Biased surface modification, ligand exchange, SAMs, kinetic analysis, well control

3.1. Introduction

Surface modification using functional ligand molecules is an effective method to determine the surface properties of a AuNP such as the dispersibility in solvent,[1] and the stimuli-responsiveness like light,[2–4] pH,[5–7] temperature.[8–15] As ligand molecules, small molecule alkanethiols have attracted much attention due to their uniform structures and small sizes compared to polymer ligands. This alkyl chain attached alkanethiols can self-assemble into highly packed and homogeneous monolayers (SAMs) providing sharp surface properties to AuNPs.[16,17] Further, surface designing the SAMs with mixed ligand molecules resulted in AuNPs obtain the hybrid surface properties and structure from these ligands,[18–21] which is supposed to be a novel and simple approach to tune surface properties by just changing the mixing ligand ratios. Nevertheless, whether surface modification proceeded as the mixing ligand ratios remain unclear.[22]

Surface modification with one kind of ligand deservedly leads to 100 % coating. On the other hand, in case of mixing modification, it is hard to guarantee the real composition of different ligands is in accord with the mixing ligand ratio for modification owing to the different properties such as amount of charge or solubility, resulting in different attachment on surface.[22] Examining the fairness/unfairness on surface modification is still an issue for researchers. Although some analytical instruments such as NMR, MS have been widely used for analyses of the real composition in SAMs, the small ligand molecules with similar structure in SAMs showing extremely low concentration are supposed to be relatively difficultly analyzed by these instruments.[23–26]

Our group have reported that AuNPs modified with thermo-responsive OEG-attached alkanethiols showed assembly/disassembly in response to a certain temperature (T_A) on dehydration/hydration state.[27] In Chapter 2, I precisely tuned the T_A via mixing two kinds of OEG-alkanethiols ligands with different termini and OEG length to tune the terminal hydrophobicity and local OEG density. Although the T_A changed along with the change in mixing ratios, the real composition on surface modification has not been accurately determined. Moreover, the biased surface modification was observed even using alkanethiols with similar structures. This phenomenon probably relates to ligand exchange. There are some reports about the ligand exchange occurred can change the composition on AuNP surface.[28–33] Claire Goldmann et al. reported that alkanethiols attaching on gold spherical nanoparticles can be replaced by the free alkanethiols in the external organic solvent.[32] Giovanni Salassa, et al. reported reports about the ligand exchange occurring on the gold nanoclusters which have broad space between immobilized inducing unpacked alkanethiols.[28] Although there are not highly packed alkanethiols SAMs formed in above reports, the effect of ligand exchange can not be ignored as biased surface modification. Moreover, it has been reported that alkanethiol SAMs can diffuse on AuNP's surface over a certain temperature and time.[34,35] Above reports suggest the alkanethiol SAMs are supposed to have the chemical activity a certain extent and the ligand exchange on AuNP surface should be investigated.

Therefore, in this study, we focus on the bias on surface modification to support the precise control of thermo-responsiveness by fair surface modification. I investigated whether ligand exchange occur by addition of alkanethiols into modified AuNPs as shown in Scheme 3-1B. Importantly, I performed kinetic analysis of ligand exchange by time course experiment to investigate how the ligand exchange influence modification

of AuNP surface. Finally, based on the investigation of ligand exchange, I preformed the surface modification with the mixed ligands in Scheme 3-1A carefully to approach to fairness by well-control of modification condition.

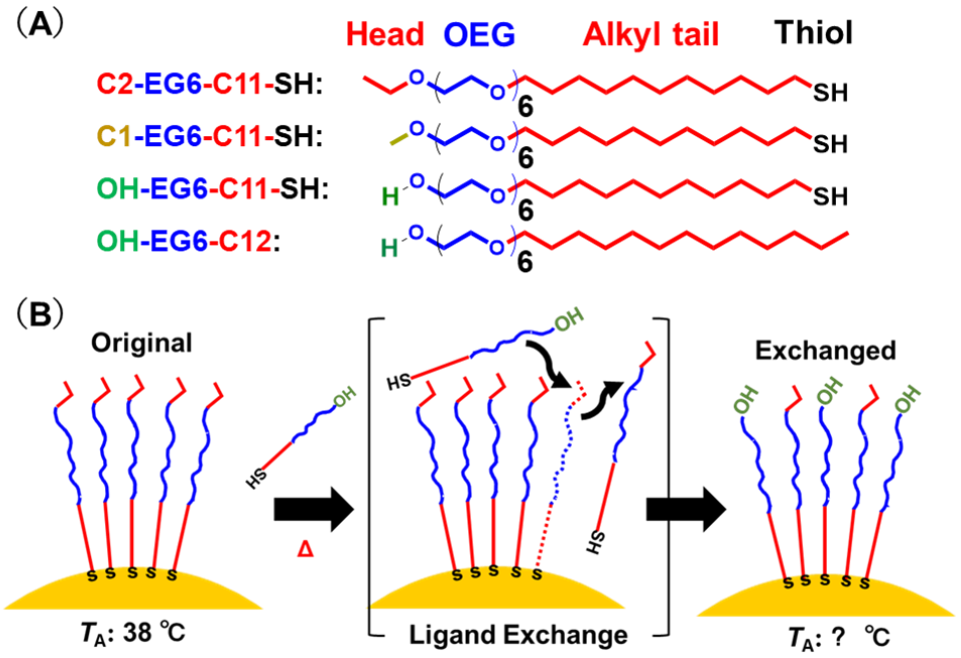

Scheme 3-1. (A) Chemical structures of the surface ligands used in this study. (B) An illustration of the change in composition on surface of nanoparticles by ligand exchange.

3-2. Experimental section

3-2-1. Materials and instruments

All commercially available reagents were used without further purification. Tris(2-carboxyethyl) phosphine (TCEP-HCl, reducing agent) was purchased from Thermo Fisher Scientific Inc. (USA). 4-(2-hydroxyethyl)-1-piperazineethanesulfonic acid (HEPES, buffer) was purchased from DOJINDO LABORATORIES (Japan). Citrate-protected AuNPs in aqueous solution (10 or 15 nm in diameter) were purchased from BBI Solutions (UK). According to the BBI Solutions Web site, AuNPs with a diameter of 10 and 15 nm have maximum coefficients of variation of 10% and 8%, respectively. Alkanethiol ligands (Scheme 3-1A) with methyl and ethyl head and alkyl-thiol tails, referred to as C1-EG6-C11-SH, C2-EG6-C11-SH, were purchased from ProChimia Surfaces, Sp.zo.o. (Poland). Alkanethiol ligands with hydroxyl head, referred to as OH-EG6-C11-SH were purchased from DOJINDO LABORATORIES. Surfactant with hydroxyl head but without thiol group, referred to as OH-EG6-C12, was purchased from Tokyo Chemical Industry Co., Ltd. (Japan). AuNPs were concentrated using a centrifuge (5430 R, Eppendorf). AuNPs were heat by a water bath (DTU-2B, TAITEC Corp.).

3-2-2. Surface modification of AuNPs

According to the method described in my previous paper,[36] the citrate protected 10 nm AuNPs were concentrated up to 94 nM by centrifugation (20,000 g for 45 min). The concentrated AuNPs (100 μL) were mixed with the aqueous solution of the alkanethiol ligand C2-EG6-C11-SH (100 μL) containing TCEP as a reductant. In this reaction, the total ligand number was adjusted to 10 equiv of Au atoms on the surface of all nanoparticles.[37] In the case of 10 nm AuNPs, the number of Au atoms on surface was calculated to be 4192/particle and the concentration of the ligand aqueous solution was set at 4 mM according to the references. For 15 nm AuNPs, it was concentrated up to 42 nM by centrifugation (14,000 g for 30 min). Moreover, the number of surface Au atoms was 9585/particle and the concentration of the ligand solution was also 4 mM. After addition of the aqueous solution of HEPES buffer (pH=8, 10mM) up to 1 mL, the AuNPs were incubated for 24 hours at 25 °C. Then, the modified AuNPs were washed 3 times by centrifugation (10 nm AuNPs: 20000g for 45 min; 15 nm AuNPs: 14000 g for 30 min), the removal of the supernatant (900 μL) and addition of HEPES buffer up to 1000 μL to remove the free ligands. The successfully modified AuNPs are referred as AuNPs@ C2-EG6-C11-SH. Surface modification with ligands C1-EG6-C11-SH, OH-EG6-C11-SH and mixed ligand were performed in same way.

3-2-3. UV−vis extinction spectroscopy

The UV−vis extinction spectra of the AuNPs were measured using a V-770 UV−vis/NIR Spectrophotometer with PAC-743R Automatic 6 position Peltier cell changer (JASCO Corp., Japan).[36] The temperature-change measurements of the AuNPs

spectra were performed at each temperature (in 5 °C intervals) with changes at a rate of 1 °C/min followed by a waiting time of 5 minutes after reaching the measurement temperature.

3-2-4. Dynamic light scattering (DLS) and zeta-potential measurement

The distribution of size and surface charge of the AuNPs were measured by Zetasizer Nano ZS (Malvern Panalytical Ltd, UK).[36] The temperature-change measurements for the AuNPs sizes were performed at each temperature are a waiting time of 2 min. The assembly temperature was defined as the middle temperature between the temperature at which the size of the AuNPs showed a significant change and the highest temperature at which the AuNPs remaining dispersed.

3-3. Results and Discussion

3.3-1. Ligand exchange on AuNPs modified with alkanethiols

I focused on whether ligand exchange occur between ligands in highly packed SAMs and existing in water. In this study, the change in thermo-responsiveness of AuNPs was adopted as proof of ligand exchange. First, I confirmed the thermo-responsiveness of AuNPs coated with alkanethiols used in this study. For instance, 10 nm AuNPs@C2-EG6-C11-SH, the obvious spectra variation indicated AuNPs showed thermo-responsive assembly between 35 and 40 ºC (Figure 3-1A left). DLS measurement showed that size distribution of AuNPs changed abruptly between 36 and 37 ºC, regarding the thermo-responsive assembly temperature (T_A) as 36.5 ºC (Figure 3-1A right). The T_A was next determined as 36.5 ± 1.0 ºC from tree independent DLS measurement. Similarly, T_A of 10 nm AuNPs@C1-EG6-C11-SH was determined to be 77.2 ± 1.2 ºC (Figure 3-1B). In the case of AuNPs@OH-EG6-C11-SH, no change in spectra and size distribution were observed within 85 ºC, meaning the T_A is over 85 ºC (Figure 3-1C). In addition, the stability of OEG-alkanethiol SAMs attaching to AuNP's surfaces was confirmed by comparation of thermo-responsiveness in repeating spectral measurement process under heating from 25 to 85 ºC. The peak wavelength of extinction spectra in every experiment temperature of 10 nm AuNPs@C2-EG6-C11-SH has been plotted as shown in Figure 3-2A. The four curves presented the similar shape and showed the same thermo-responsive assembly between 35 and 40 ºC. Moreover, DLS analysis after 4 times heating up to 85 ºC showed the T_A of 38 ºC (Figure 3-2B), which is same with AuNPs without repeating measurement. This unchanged T_A indicated OEG-alkanethiol hardly detached from AuNP surface on heat.

Next, I added the free alkanethiols OH-EG6-C11-SH into the 10 nm AuNPs@C2-EG6-C11-SH and then measured the thermo-responsiveness by extinction spectra (from 25 to 85 ºC) and DLS. Although the good attachment of OEG-alkanethiol SAMs on AuNP surface has been confirmed, ligand exchange between C2-EG6-C11-SH on surface and the free OH-EG6-C11-SH in water was observed on same heating process. As shown in Figure 3-3A and 3-5, green line, extinction spectra and peak wavelength on heating presented the thermo-responsive assembly between 35 and 40 ºC, but disassembly between 60 and 65 ºC. Finally, this extinction peak returned to the original state. After removal of free ligands via purification by 3 times, spectra showed no shift in any temperature, meaning AuNPs stayed in dispersion condition (Figure 3-3B and 3-5, orange line). DLS analysis showed that AuNPs didn't assemble within 85 ºC (Figure 3-3C). It indicated that the thermo-responsiveness has been changed by addition of free alkanethiols ligands on heating. On the other hand, OH-EG6-C12 with the similar structure to OH-EG6-C11-SH ligand but without thiol group was added into AuNPs@ C2-EG6-C11-SH showing the same thermo-responsiveness (Figure 3-5, blue line) with original AuNPs (Figure 3-5, red line). That is assembly between 35 ºC and 40 ºC (Figure 3-4A) and the unchanged T_A of 38 ºC (Figure 3-4B). Compared with OH-EG6-C11-SH and OH-EG6-C12, only the molecules OH-EG6-C11-SH having thiol group can change the thermo-responsiveness of AuNPs@C2-EG6-C11-SH. These indicated that the free alkanethiols OH-EG6-C11-SH replaced with the C2-EG6-C11-SH on surface of AuNPs on heating, resulting in the rearrangement in surface hydrophobicity to change thermo-responsiveness of AuNPs. In the same way, addition of C1-EG6-C11-SH also caused the change in thermo-responsiveness of AuNPs@C2-EG6-C11-SH, which showed the thermo-responsive assembly between 55 and 60 ºC (Figure 3-6A and

3-6C, green line) and located at between AuNPs@C2-EG6-C11-SH (Figure 3-6C, blue line) and AuNPs@C1-EG6-C11-SH (Figure 3-6C, red line). Similarly, DLS analyses showed T_A of 52 ºC (Figure 3-6B), which is higher than AuNPs@ C2-EG6-C11-SH (38 ºC) but lower than AuNPs@ C1-EG6-C11-SH (77 ºC). These indicated that the free alkanethiol ligand C1-EG6-C11-SH replaced with immobilized C2-EG6-C11-SH, resulting in the changes in the composition of SAMs, like the surface modification with mixed ligand to control SAMs' composition.

To further confirm the free alkanethiols replace the immobilized ligands on surface, those samples of AuNPs@ C2-EG6-C11-SH after reaction with OH-EG6-C11-SH (Figure 3-7A -iii) were purified 3 times, mixed with C2-EG6-C11-SH (300 μM) as free ligands, and then heated at 85 ºC for 30 minutes (Figure 3-7A-iii). DLS measurement showed T_A changed from immeasurable value (>90 ºC) (Figure 3-7B-ii) to 41 ºC (Figure 3-7B-iii), which almost returned to the original T_A of 38 ºC (Figure 3-7B-i) by addition of C2-EG6-C11-SH on heating. The recovery of T_A suggested that the free ligand OH-EG6-C11-SH replaced with the immobilized C2-EG6-C11-SH on surface, resulting in huge increase of the T_A, and then the addition of C2-EG6-C11-SH replaced with the immobilized OH-EG6-C11-SH in turn causing the recover to the T_A (Figure 7 and 8). It indicated that the immobilized alkanethiol ligands on AuNPs' surface can be replaced by free alkanethiol ligands in external aqueous solution even though they have formed the stable and highly packed SAMs.

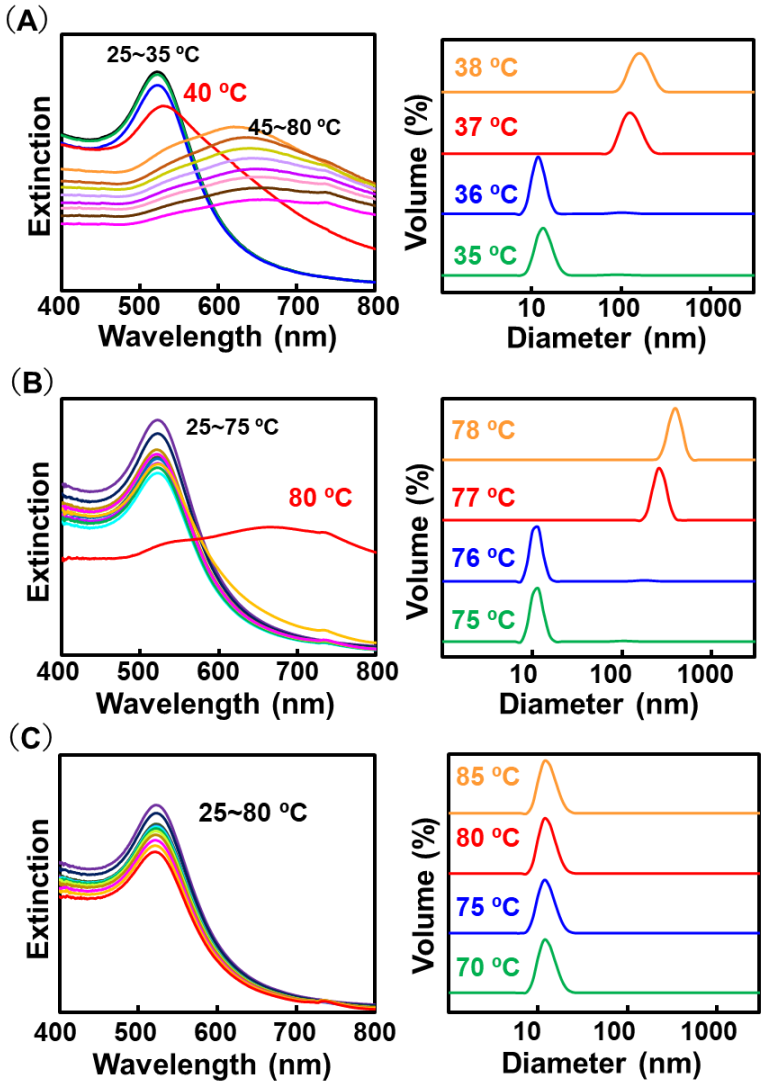

Figure 3-1. Thermo-responsive phenomena of 10 nm AuNPs modified with (A) C2-EG6-C11-SH, (B) C1-EG6-C11-SH, (C) OH-EG6-C11-SH ligands. Left: extinction spectra and right: size distribution.

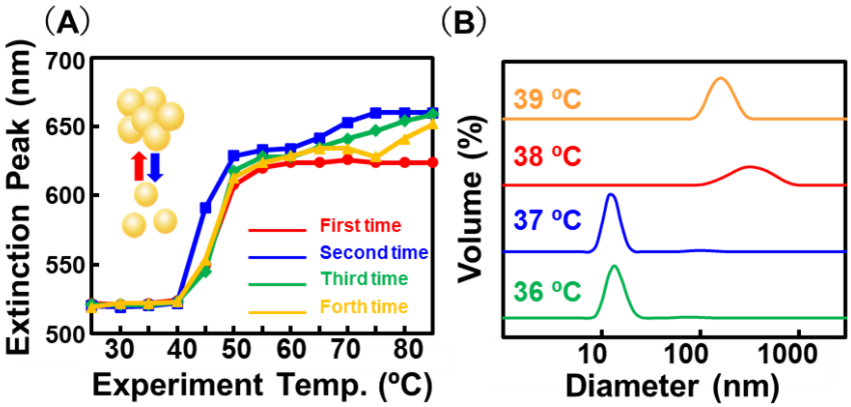

Figure 3-2. (A) Temperature-dependent changes in the extinction peak wavelength of 10 nm AuNPs @ C2-EG6-C11-SH for four repeating cycles during heating process. (B) Size distribution of AuNPs measured by DLS after four repeating measurement of extinction spectra

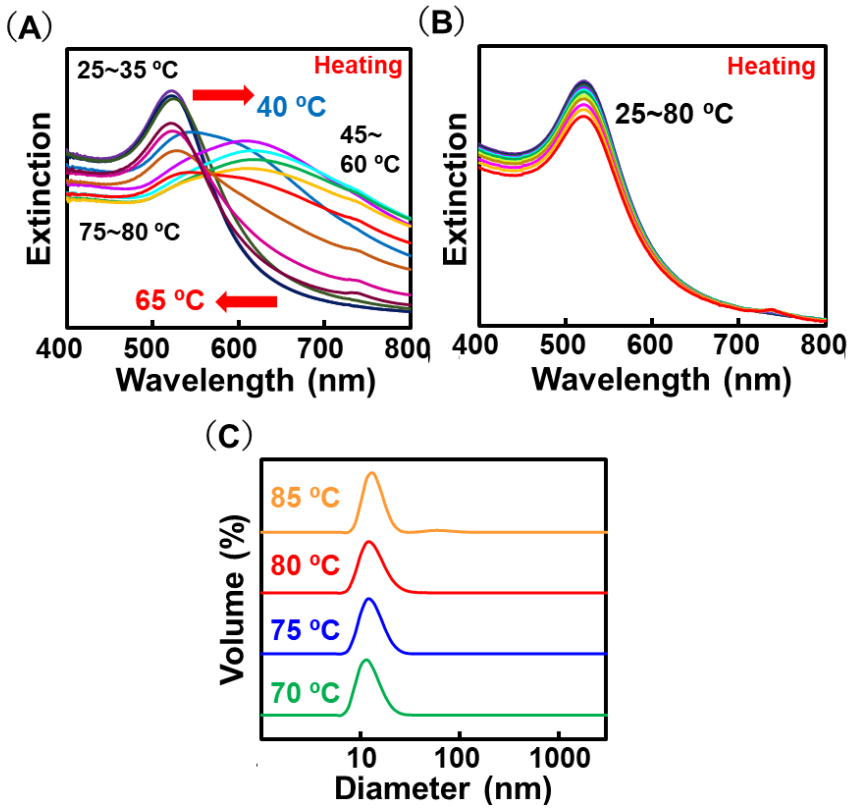

Figure 3-3. Thermo-responsive phenomena of AuNPs modified with C2-EG6-C11-SH by addition of OH-EG6-C11-SH: (A) Measurement with free ligands, (B) Measurement after removal of free ligands. (C) Size distribution of 10 nm AuNPs@ C2-EG6-C11-SH by addition of OH-EG6-C11-SH.

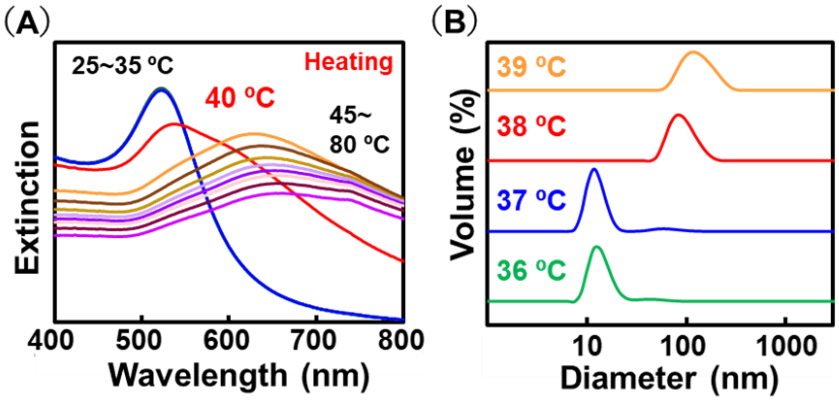

Figure 3-4. Thermo-responsive phenomena of AuNPs modified with C2-EG6-C11-SH by addition of OH-EG6-C12: (A) Extinction spectra, (B) Size distribution.

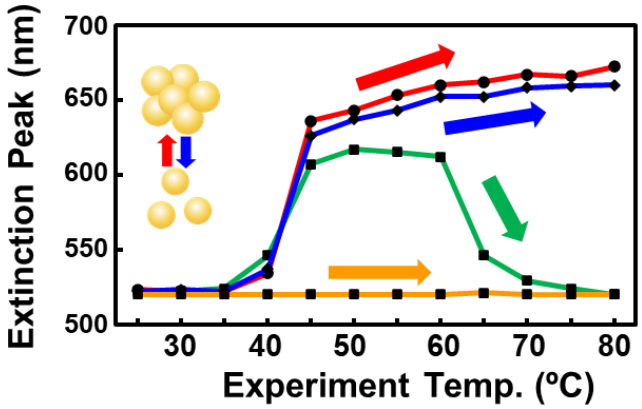

Figure 3-5. Temperature-dependent changes in the extinction peak wavelength of 10 nm AuNPs @ C2-EG6-C11-SH: without free ligands (red), with OH-EG6-C12 addition (blue), with OH-EG6-C11-SH addition (green), removal of free OH-EG6-C12-SH (orange).

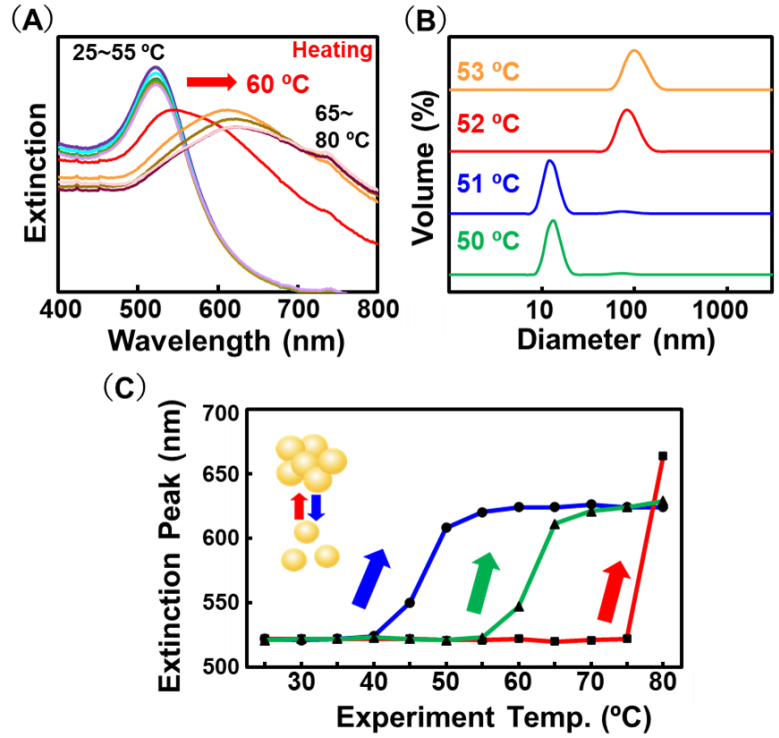

Figure 3-6. Thermo-responsive phenomena of AuNPs modified with C2-EG6-C11-SH by addition of C1-EG6-C11-SH: (A) Extinction spectra, (B) Size distribution. (C) Temperature-dependent changes in the extinction peak wavelength of 10 nm AuNPs modified with C2-EG6-C11-SH (blue), with C2-EG6-C11-SH by addition of C1-EG6-C11-SH (green), with C1-EG6-C11-SH addition (red).

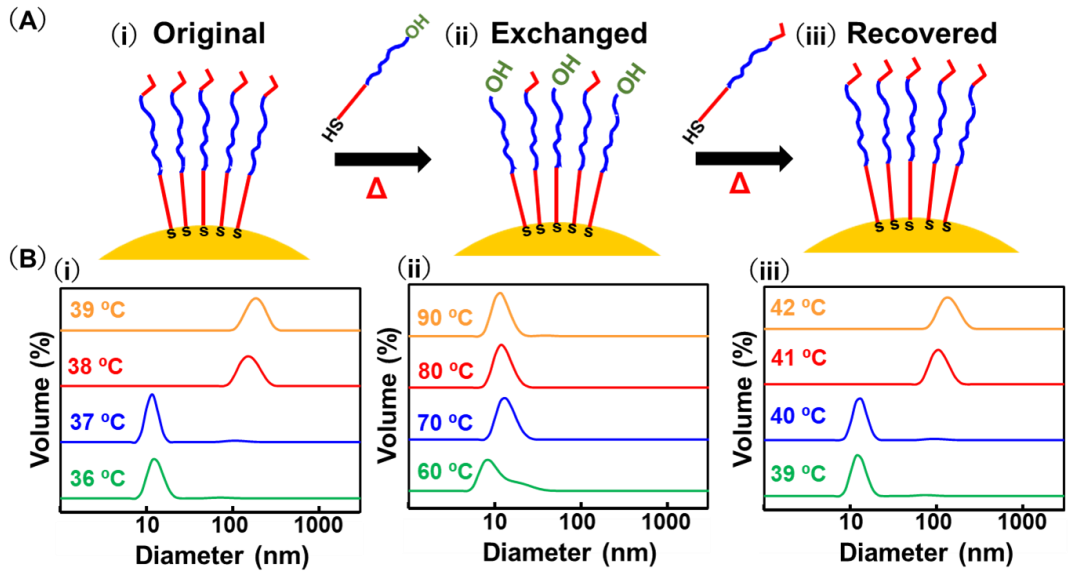

Figure 3-7. (A) An illustration and (B) the DLS size distribution of every step during ligand exchange. (i) Original10 nm AuNPs @ C2-EG6-C11-SH, (ii) 10 nm AuNPs @ C2-EG6-C11-SH exchanged by OH-EG6-C11-SH; (iii) AuNPs @ C2-EG6-C11-SH recovered by addition of C2-EG6-C11-SH.

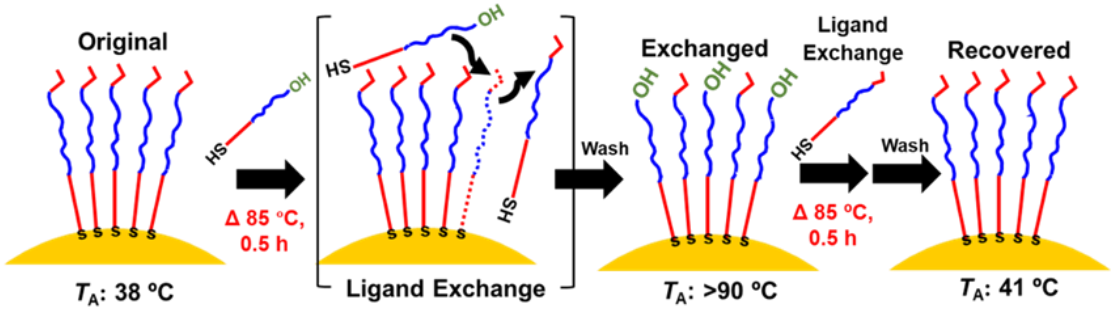

Figure 3-8. An illustration of ligand exchange between alkanethiol ligands in and outside SAMs.

3-3-2. Kinetic analyses of ligand exchange

To confirm how the ligand exchange have an effect on the composition of AuNP surface in various experimental condition, the kinetic analyses of ligand exchange reaction were performed. 10 nm AuNPs@ OH-EG6-C11-SH mixed with free C2-EG6-C11-SH (75 μM) was heated at 85 ºC, 55 ºC and 25 ºC for 3, 5, 30, 60, 180, 1440 mins and 1, 2, 3, 4, 5 days, respectively. As shown in Figure 3-9A, T_A of AuNPs dramatically decreased only 5 mins passed at 85 ºC, indicating the speed of ligand exchange reaction between C2-EG6-C11-SH and OH-EG6-C11-SH was extremely quick. Importantly, the assembly temperature exactly located in the range of estimation value (45~55 ºC). This value was calculated from the ratios of each ligand on concentration in reaction medium combining with the relation curve between surface ligand ratios and assembly temperature as mentioned in Chapter 2. Above suggested that the ligand exchange proceeded as the ratios of each ligand in medium at first. It can be explained from the perspective of reaction kinetics. Ligand exchange is expected to be divided into the attachment and detachment of C2-EG6-C11-SH or OH-EG6-C11-SH. The ability of attachment to AuNPs of each ligand should be equal due to the similar structures. However, at first, only free C2-EG6-C11-SH existed in external solutions. According to the reaction kinetics, the rate of chemical combination (ligand attachment to AuNPs) is concentration-dependent and the rate of chemical division (ligand detachment from AuNPs) is basically concentration independent, promoting C2-EG6-C11-SH quickly attached to AuNPs and the equivalent OH-EG6 detached from AuNPs as shown in Figure 3-10. Along with the reaction time passed, T_A began to increase on the contrary. The decrease then increase of T_A indicated some detached OH-EG6-C11-SH which was

replaced with C2-EG6-C11-SH have returned to the AuNP surface. According to stable systems only in lowest-energy state, it seems that the energetic stability on AuNPs of OH-EG6-C11-SH is much stronger than C2-EG6-C11-SH. Therefore, when the attachment of C2-EG6-C11-SH reached the saturation quickly, the detachment of C2-EG6-C11-SH from AuNPs competed against the immobilized OH-EG6-C11-SH. Since the rate of ligand detachment is concentration independent but molecular mobility-dependent, C2-EG6-C11-SH with the weaker energetic stability on AuNP detached from AuNP surface in the end and equivalent OH-EG6 returned. The return of replaced ligands over time suggest that composition of SAMs on AuNP surface is not always invariable. On the other hand, AuNPs@C2-EG6-C11-SH mixed with free OH-EG6-C11-SH turned into no thermo-responsiveness (T_A > 90 ºC) just 5 mins passed but the recovery of thermo-responsiveness wasn't observed within 3 h (Figure 3-9B), emphasizing the unfairness on ligand exchange between OH-EG6-C11-SH and C2-EG6-C11-SH. In the same way, 10 nm AuNPs@ C1-EG6-C11-SH added by C2-EG6-C11-SH also showed a sharp decrease in T_A at 85 ºC followed by a slow increase in T_A and reached to the equilibrium state after 3 h (Figure 3-9C). The slight recovery of T_A also indicated a few C1-EG6C11-SH have returned to the AuNPs. On the other hand, 10 nm AuNPs@ C2-EG6-C11-SH added by C1-EG6-C11-SH showed a drastically increased firstly but continued to rise slowly on T_A within 3 h, meaning the external C1-EG6-C11-SH kept replacing with the immobilized C2-EG6-C11-SH and these detached C2-EG6-C11-SH didn't return to AuNPs (Figure 3-9D). These suggested that the slightly unfair ligand exchange is possible to exist between C2-EG6-C11-SH and C1-EG6-C11-SH. These reactions mostly showed ligand exchange proceeded on the ratio of ligands in reaction medium firstly then showed the unfairness on ligand exchange

over time, suggesting the traditional viewpoint about longer time and better surface modification is not appropriate.

Figure 3-11 showed the T_A in time course of 10 nm AuNPs@ C1-EG6-C11-SH after addition of C2-EG6-C11-SH at 85 ºC, 55 ºC and 25 ºC. The speed of attachment stage of ligand exchange increased along with the improvement of temperature as expected due to the effect of temperature on reaction constant. Although AuNPs at higher temperature showed faster ligand exchange, they all reached the similar equilibrium state over time, suggesting the temperature only have an effect on rate constant whereas the equilibrium constant of ligand exchange. It can explain that the ligand exchange still occurs even at room temperature (25 ºC) but it proceeded slowly and is supposed to take longer time to reach the equilibrium constant. Although, it is difficult to figure out when the ligand exchanges start to take effect (at the same time with surface modification or after modification), reducing reaction time and decreasing reaction temperature are supposed to slow down the ligand exchange especially appearance of possible cause of unfairness and provide a more favorable environment for surface modification.

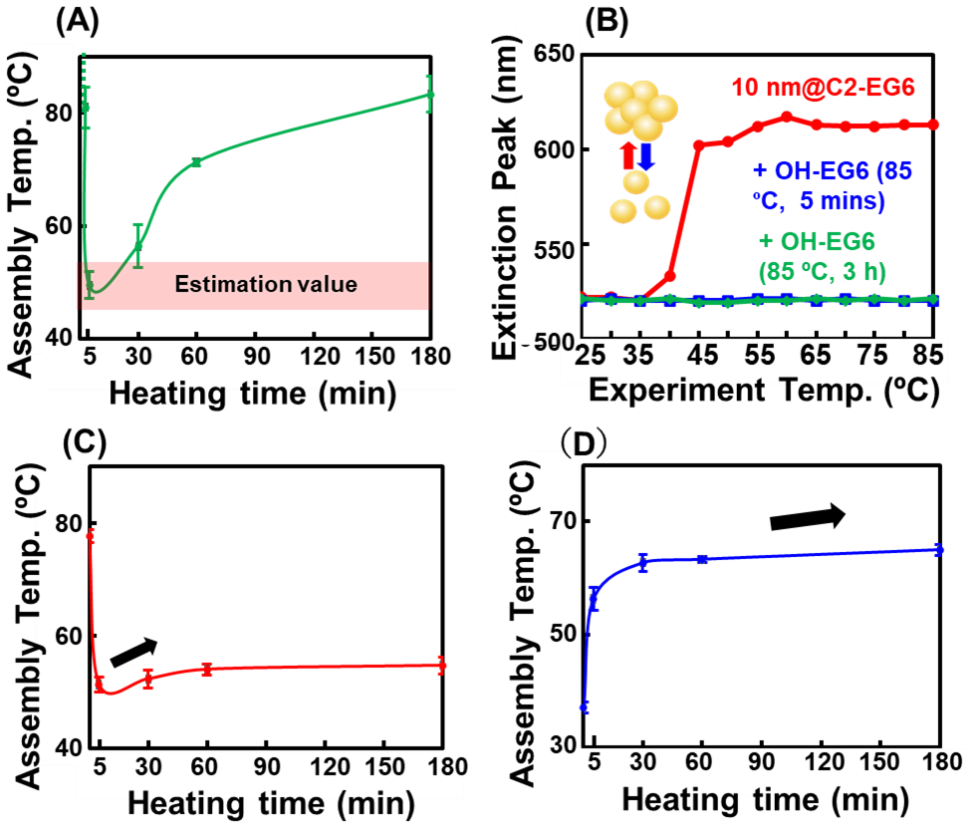

Figure 3-9. Time variation of thermo-responsiveness of 10 nm AuNPs @ (A) OH-EG6C11-SH by addition of C2-EG6C11-SH, (C) C1-EG6-C11-SH by addition of C2-EG6C11-SH, (D) C2-EG6-C11-SH by addition of C1-EG6C11-SH at 85 ℃. (B) Temperature-dependent changes in the extinction peak wavelength of 10 nm AuNPs modified with C2-EG6-C11-SH (red); by addition of C1-EG6-C11-SH and heated at 85 ℃, 5 mins (blue), at 85 ℃, 3 h (green).

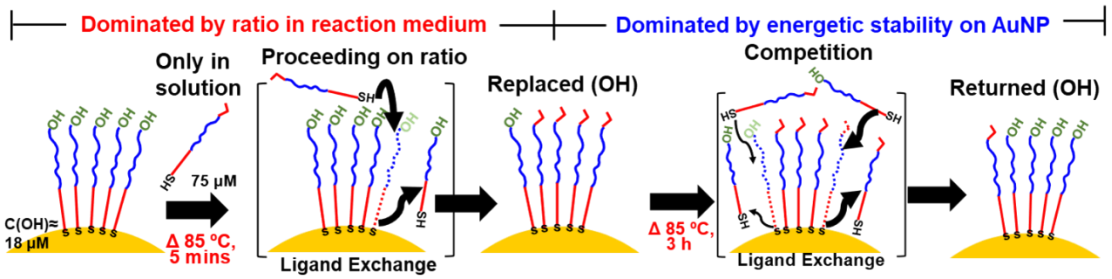

Figure 3-10. An illustration of ligand exchange between OH-EG6-C11-SH and C2-EG6-C11-SH in time course experiment

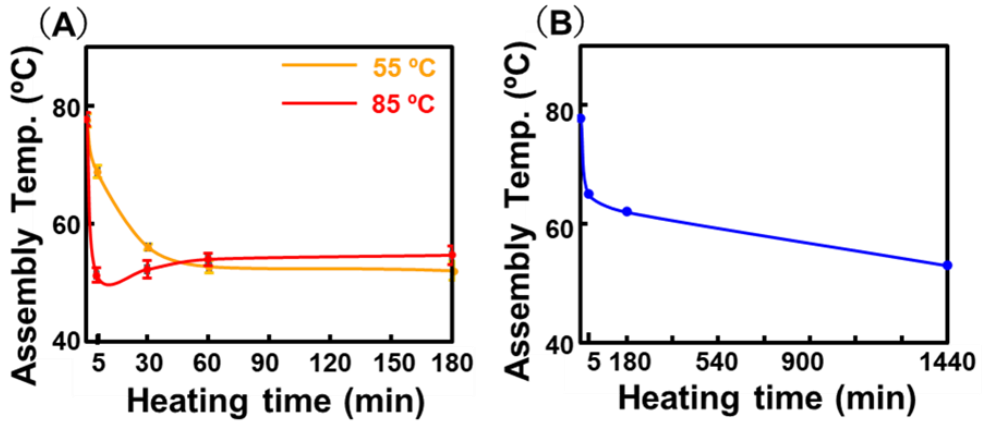

Figure 3-11. Time variation of assembly temperature of 10 nm AuNPs @ C1-EG6-C11-SH by addition of C2-EG6-C11-SH at the ligand exchange temperature of (A) 85 and 55 ºC, (B) 25 ºC.

3-3-3. Unfairness on ligand exchange

To confirm the unfairness on ligand exchange, 10 nm AuNPs modified with equally mixed ligand (C2-EG6-C11-SH and OH-EG6-C11-SH) were prepared. In this study, the surface modification was set to the shorter reaction time and lower reaction temperature as 25 ºC, 24 h. After modification, the same equally mixed ligands (75 μM) were added into this AuNP (Scheme 3-2). This AuNP was heated at 85 ºC, 3 hours and then purified by 3 times. Each T_A determined by DLS measurement was summarized in Figure 3-12A, 10 nm AuNPs@ (50 % C2-EG6-C11-SH + 50 % OH-EG6-C11-SH) assembled at 74 ºC, but these AuNPs turned into disassembly within 90 ºC by addition of mixed ligands. On the other hand, 10 nm AuNPs@ (50 % C2-EG6-C11-SH + 50 % C1-EG6-C11-SH) slightly shift from 54 ºC to 53 ºC by addition of the equally mixed ligands, regarding as almost unchanged (Figure 3-12B). The unchanged assembly temperature of C1-EG6-C11-SH mixed C2-EG6-C11-SH after ligand addition indicated that 25 ºC, 24 h is enough for surface modification using our OEG-alkanethiols. Nevertheless, whether the unfair ligand exchange between C1-EG6-C11-SH and C2-EG6-C11-SH have occurred is unclear. On the other hand, the great changes in T_A of modification with OH-EG6-C11-SH and C2-EG6-C11-SH suggested the free OH-EG6-C11-SH preferred to replace the immobilized C2-EG6-C11-SH. That means the unfair ligand exchange occurred assuredly, resulting in the increase on T_A. The difference in unfairness on ligand exchange of these alkanethiols at same experimental condition can be explained by the ligand exchange activity that OH-EG6-C11-SH replacing C2-EG6-C11-SH is much stronger than C1-EG6-C11-SH replacing C2-EG6-C11-SH (Figure 3-13). Furthermore, these small differences in molecular structure such as change in

terminal hydrophobicity have a great effect on ligand exchange activity. In addition, 25 ^{o}C, 24 h is a good experimental condition for surface modification.

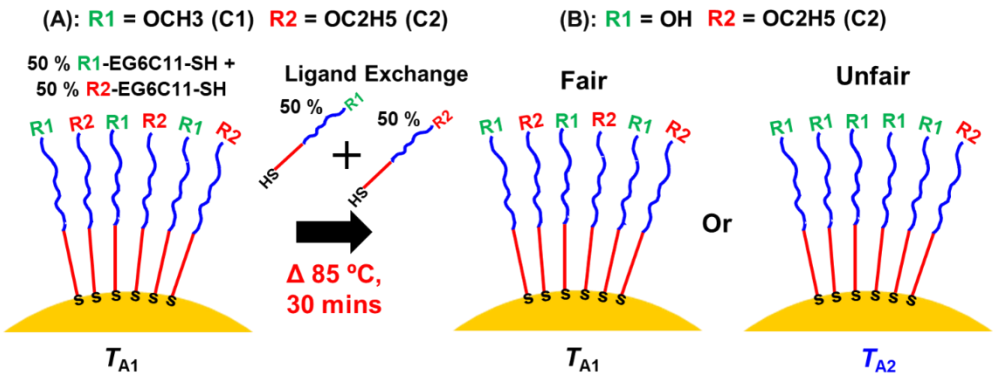

Scheme 3-2. Investigation of unfair ligand exchange: (A) 10 nm AuNPs @ (50 % C1-EG6-C11-SH + 50 % C2-EG6-C11-SH) by addition of free ligands (50 % C1-EG6-C11-SH + 50 % C2-EG6-C11-SH); (B) 10 nm AuNPs @ (50 % OH-EG6-C11-SH + 50 % C2-EG6-C11-SH) by addition of free ligands (50 % OH-EG6-C11-SH + 50 % C2-EG6-C11-SH)

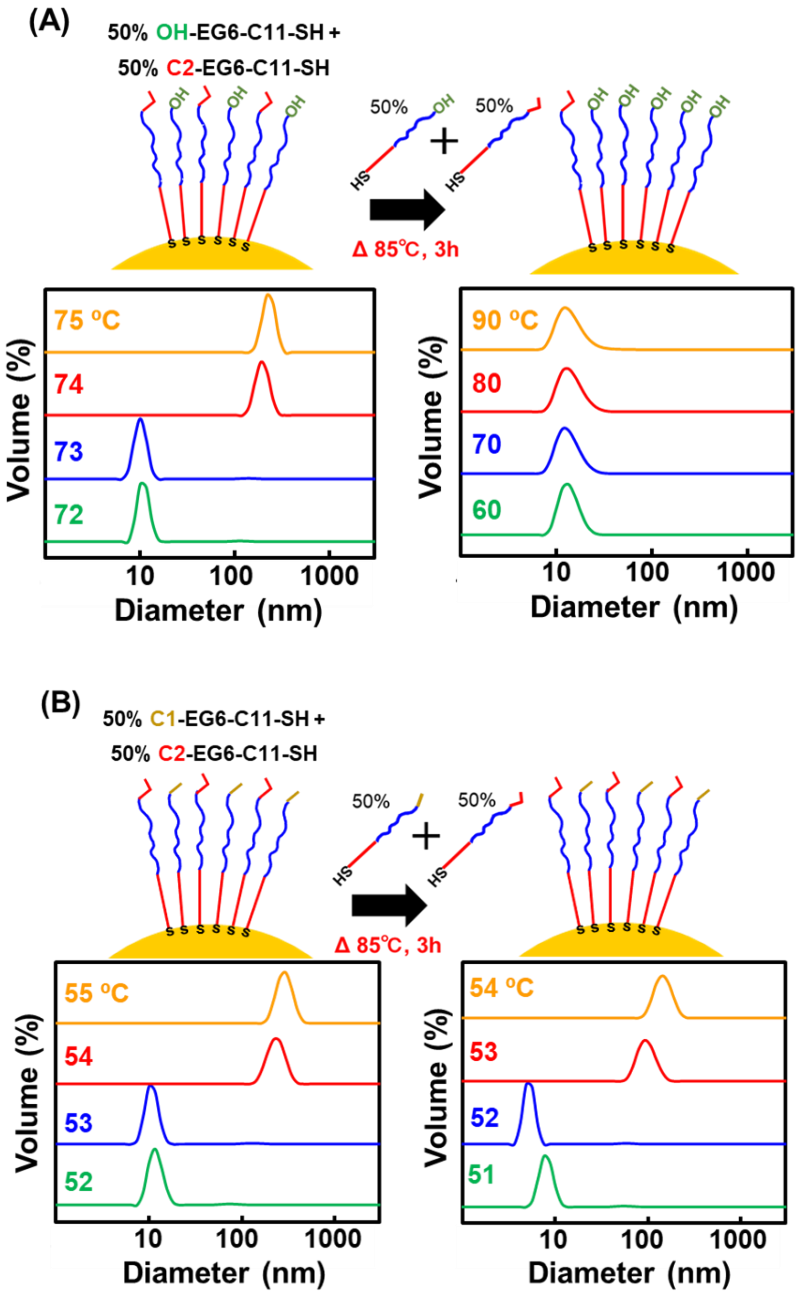

Figure 3-12. An illustration (top) and the size distribution (down) of (A) 10 nm AuNPs @ (50 % C2-EG6-C11-SH + 50 % OH-EG6-C11-SH) before (left) and after (right) addition of free ligands (50% OH-EG6-C11-SH + 50% C2-EG6-C11-SH) and 10 nm AuNPs @ (50 % C2-EG6-C11-SH + 50 % C1-EG6-C11-SH) before (left) and after (right) addition of free ligands (50% C1-EG6-C11-SH + 50% C2-EG6-C11-SH)

3-3-4. Fair surface modification via well-control of modification conditions

In this study, all 10 nm AuNPs was modified with alkanethiols as shown in Scheme 3-1A and modification under 25 ºC, 24 h followed by purification and measurement of thermo-responsiveness via extinction spectra and size distribution. There are obvious shifts in T_A between 36.5 ºC for 100 % C2-EG6C11-SH and 77.2 ºC for 100 % C1-EG6-C11-SH, suggesting it is possible to tune the T_A by controlling the composition of these ligands mixing ratios, which is similar to our previous report.[36] I prepared AuNPs modified with C2-EG6C11-SH and C1-EG6-C11-SH at various mixing ratio and their thermo-responsiveness were determined as shown in Table 3-1 and Figure 3-13A. Following, to summarize the relationships among these T_A in various mixing ratio, curve fitting was performed. C2-EG6-C11-SH mixed with C1-EG6-C11-SH showed the standard linear relationship and good R^2, which is the square of the correlation coefficient between the actual and predicted Y values. It indicated that the real composition of alkanethiols on AuNP surface was almost in accord with the mixing ligand ratio for surface modification, meaning it is possible to restrain the biased surface modification by well-control of reaction condition. Similarly, C2-EG6-C11-SH mixed with OH-EG6-C11-SH also conformed to liner relationship and good R^2 (Figure 3-13B). Interestingly, the tiny difference in R^2 of curve fitting of C1-EG6-C11-SH / C2-EG6-C11-SH (0.998) and OH-EG6-C11-SH / C2-EG6-C11-SH (0.976) was observed. It is supposed to be caused by different ligand exchange activity and seems that unfairness on ligand exchange still influence slightly the surface modification. In this study, although the relationship between ligand exchange and surface modification is still unclear, I have made a breakthrough of approach to the fair surface ligand exchange by well-control of modification condition compared with the former bias modification,[36]

which contribute to the precise control thermo-responsiveness by fair surface modification.

Table 3-1. Assembly temperature of 10 nm AuNPs modified with mixed ligands: (A) C1-EG6-C11-SH and C2-EG6-C11-SH; (B) OH-EG-6C11-SH and C2-EG-6C11-SH.

(**A**)

C2-EG6 : C1-EG6 Ligand Ratio	Assembly *1 Temperature (ºC)	S. D.
75 : 25	45.2	1.2
50 : 50	55.5	1.7
25 : 75	65.5	1.0

(**B**)

C2-EG6 : OH-EG6 Ligand Ratio	Assembly *1 Temperature (ºC)	S. D.
50 : 50	74.3	2.6
60 : 40	63.2	2.5
70 : 30	54.8	2.1
80 : 20	46.5	1.0
90 : 10	40.2	0.6

*1 T_A was from three independent DLS analysis.

.

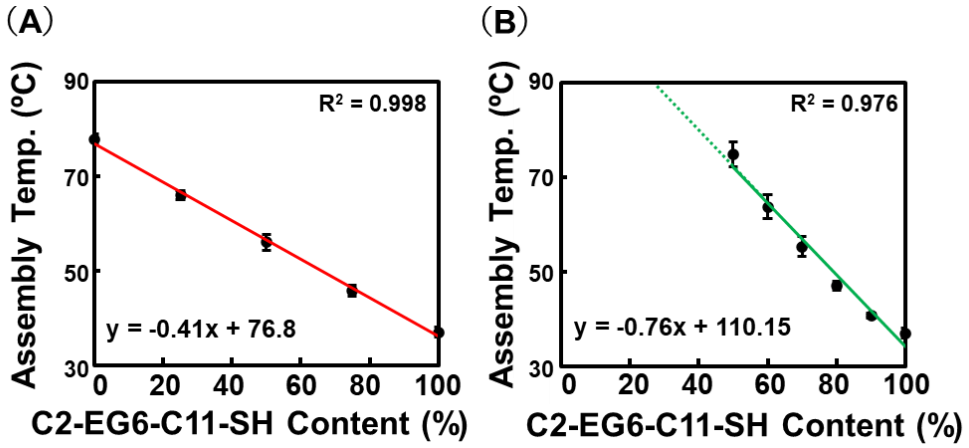

Figure 3-13. Assembly temperature of 10 nm AuNPs modified with a mixture of (A) C2-EG6-C11-SH and C1-EG6-C11-SH, (B) C2-EG6-C11-SH and OH-EG6-C11-SH. x refers to the ratio of C2-EG6-C11-SH and y refers to the T_A of AuNPs. Error bars represent S.D. (n=3).

3-4. Conclusion

In this study, ligand exchange between ligands in self-assembled monolayer (SAMs) on AuNP surface and existing in solution was proved to occur. This ligand exchange was supposed to proceed on the ratio of each ligand in the reaction medium firstly and then showed the unfairness on ligand exchange over time corresponding to the bias on surface modification. This unfairness is in related to the tiny difference in structure at the termini of alkanethiols such as hydrophobicity at terminus. Nevertheless, the unfairness on surface modification was expected to be restrained and surface modification can proceed as the ratios of mixed ligands with similar structure by well-control of experiment condition such as modification time and temperature.

Although, it remains unclear how much unfairness on ligand exchange contributes to the bias surface modifications, this study is supposed to provide an important reference for surface modification. Thermo-responsiveness reprogrammed by addition of free alkanethiols in this study provides a novel molecular design to the tuning of their surface properties based on the controllable ligand exchange. In addition, the interesting phenomenon about the drastic change and recovery of assembly temperature by time course experiment reflect the special behavior of ligands on interface between AuNP surface and solution during ligand exchange reaction, supposing to open a door for studying the ligand exchange in molecular level.

3-5. Reference

(1) Andala, D. M.; Shin, S. H. R.; Lee, H. Y.; Bishop, K. J. M. Templated Synthesis of Amphiphilic Nanoparticles at the Liquid-Liquid Interface. *ACS Nano* **2012**, *6* (2), 1044–1050.

(2) Niehues, M.; Tegeder, P.; Ravoo, B. J. Reversible End-to-End Assembly of Selectively Functionalized Gold Nanorods by Light-Responsive Arylazopyrazole-Cyclodextrin Interaction. *Beilstein J. Org. Chem.* **2019**, *15*, 1407–1415.

(3) Chen, Y.; Wang, Z.; He, Y.; Yoon, Y. J.; Jung, J.; Zhang, G.; Lin, Z. Light-Enabled Reversible Self-Assembly and Tunable Optical Properties of Stable Hairy Nanoparticles. *Proc. Natl. Acad. Sci. U. S. A.* **2018**, *115* (7), E1391–E1400.

(4) Kundu, P. K.; Samanta, D.; Leizrowice, R.; Margulis, B.; Zhao, H.; Börner, M.; Udayabhaskararao, T.; Manna, D.; Klajn, R. Light-Controlled Self-Assembly of Non-Photoresponsive Nanoparticles. *Nat. Chem.* **2015**, *7* (8), 646–652.

(5) Gao, W.; Chan, J. M.; Farokhzad, O. C. Reviews PH-Responsive Nanoparticles for Drug Delivery. **2010**, *7* (6), 1913–1920.

(6) Orendorff, C. J.; Hankins, P. L.; Murphy, C. J. PH-Triggered Assembly of Gold Nanorods. *Langmuir* **2005**, *21* (5), 2022–2026.

(7) Torii, Y.; Sugimura, N.; Mitomo, H.; Niikura, K.; Ijiro, K. PH-Responsive Coassembly of Oligo(Ethylene Glycol)-Coated Gold Nanoparticles with External Anionic Polymers via Hydrogen Bonding. *Langmuir* **2017**, *33* (22), 5537–5544.

(8) Poudel, A. J.; He, F.; Huang, L.; Xiao, L.; Yang, G. Supramolecular Hydrogels Based on Poly (Ethylene Glycol)-Poly (Lactic Acid) Block Copolymer Micelles and α-Cyclodextrin for Potential Injectable Drug Delivery System. *Carbohydr. Polym.* **2018**, *194* (April), 69–79.

(9) Housni, A.; Zhao, Y. Gold Nanoparticles Functionalized with Block Copolymers Displaying Either LCST or UCST Thermosensitivity in Aqueous Solution. *Langmuir* **2010**, *26* (15), 12933–12939.

(10) Tomczyk, E.; Promiński, A.; Bagiński, M.; Górecka, E.; Wójcik, M. Gold Nanoparticles Thin Films with Thermo- and Photoresponsive Plasmonic Properties Realized with Liquid-Crystalline Ligands. *Small* **2019**, *15* (37), 1–8.

(11) Yu, J.; Ha, W.; Sun, J. N.; Shi, Y. P. Supramolecular Hybrid Hydrogel Based on Host-Guest Interaction and Its Application in Drug Delivery. *ACS Appl. Mater. Interfaces* **2014**, *6* (22), 19544–19551.

(12) Liu, G.; Wang, D.; Zhou, F.; Liu, W. Electrostatic Self-Assembly of Au Nanoparticles onto Thermosensitive Magnetic Core-Shell Microgels for Thermally Tunable and Magnetically Recyclable Catalysis. *Small* **2015**, *11* (23), 2807–2816.

(13) Zhu, M. Q.; Wang, L. Q.; Exarhos, G. J.; Li, A. D. Q. Thermosensitive Gold Nanoparticles. *J. Am. Chem. Soc.* **2004**, *126* (9), 2656–2657.

(14) Bessa, P. C.; Machado, R.; Nürnberger, S.; Dopler, D.; Banerjee, A.; Cunha, A. M.; Rodríguez-Cabello, J. C.; Redl, H.; van Griensven, M.; Reis, R. L.; et al. Thermoresponsive Self-Assembled Elastin-Based Nanoparticles for Delivery of BMPs. *J. Control. Release* **2010**, *142* (3), 312–318.

(15) Liu, Y.; Han, X.; He, L.; Yin, Y. Thermoresponsive Assembly of Charged Gold Nanoparticles and Their Reversible Tuning of Plasmon Coupling. *Angew. Chemie - Int. Ed.* **2012**, *51* (26), 6373–6377.

(16) Sashikata, K.; Sugata, T.; Sugimasa, M.; Itaya, K. In Situ Scanning Tunneling Microscopy Observation of a Porphyrin Adlayer on an Iodine-Modified Pt(100) Electrode. *Langmuir* **1998**, *14* (10), 2893–2902.

(17) Love, J. C.; Estroff, L. A.; Kriebel, J. K.; Nuzzo, R. G.; Whitesides, G. M. *Self-Assembled Monolayers of Thiolates on Metals as a Form of Nanotechnology*; 2005; Vol. 105.

(18) Liu, X.; Li, H.; Jin, Q.; Ji, J. Surface Tailoring of Nanoparticles via Mixed-Charge Monolayers and Their Biomedical Applications. *Small* **2014**, *10* (21), 4230–4242.

(19) Eshhar, Z.; Reiter, Y.; Sivan, U. Controlled Platform for Studying Cell − Ligand Interactions. *Nano Lett.* **2012**, *12*, 4992.

(20) Ghorai, P. K.; Glotzer, S. C. Atomistic Simulation Study of Striped Phase Separation in Mixed-Ligand Self-Assembled Monolayer Coated Nanoparticles. *J. Phys. Chem. C* **2010**, *114* (45), 19182–19187.

(21) Petrie, T. A.; Stanley, B. T.; García, A. J. Micropatterned Surfaces with Controlled Ligand Tethering. *J. Biomed. Mater. Res. A* **2009**, *90* (3), 755–765.

(22) Şologan, M.; Cantarutti, C.; Bidoggia, S.; Polizzi, S.; Pengo, P.; Pasquato, L. Routes to the Preparation of Mixed Monolayers of Fluorinated and Hydrogenated Alkanethiolates Grafted on the Surface of Gold Nanoparticles. *Faraday Discuss.* **2016**, *191*, 527–543.

(23) Harkness, K. M.; Balinski, A.; McLean, J. A.; Cliffel, D. E. Nanoscale Phase Segregation of Mixed Thiolates on Gold Nanoparticles. *Angew. Chemie - Int. Ed.* **2011**, *50* (45), 10554–10559.

(24) Wu, M.; Vartanian, A. M.; Chong, G.; Pandiakumar, A. K.; Hamers, R. J.; Hernandez, R.; Murphy, C. J. Solution NMR Analysis of Ligand Environment in Quaternary Ammonium-Terminated Self-Assembled Monolayers on Gold Nanoparticles: The Effect of Surface Curvature and Ligand Structure. *J. Am. Chem. Soc.* **2019**, *141* (10), 4316–4327.

(25) Liu, X.; Yu, M.; Kim, H.; Mameli, M.; Stellacci, F. Determination of Monolayer-Protected Gold Nanoparticle Ligand-Shell Morphology Using NMR. *Nat. Commun.* **2012**, *3*.

(26) Retout, M.; Brunetti, E.; Valkenier, H.; Bruylants, G. Limits of Thiol Chemistry Revealed by Quantitative Analysis of Mixed Layers of Thiolated-PEG Ligands Grafted onto Gold Nanoparticles. *J. Colloid Interface Sci.* **2019**, *557*, 807–815.

(27) Iida, R.; Mitomo, H.; Matsuo, Y.; Niikura, K.; Ijiro, K. Thermoresponsive Assembly of Gold Nanoparticles Coated with Oligo(Ethylene Glycol) Ligands with an Alkyl Head. *J. Phys. Chem. C* **2016**, *120* (29), 15846–15854.

(28) Salassa, G.; Sels, A.; Mancin, F.; Bürgi, T. Dynamic Nature of Thiolate Monolayer in Au25(SR)18 Nanoclusters. *ACS Nano* **2017**, *11* (12), 12609–12614.

(29) Niihori, Y.; Kikuchi, Y.; Kato, A.; Matsuzaki, M.; Negishi, Y. Understanding Ligand-Exchange Reactions on Thiolate-Protected Gold Clusters by Probing

Isomer Distributions Using Reversed-Phase High-Performance Liquid Chromatography. *ACS Nano* **2015**, *9* (9), 9347–9356.

(30) Smith, A. M.; Marbella, L. E.; Johnston, K. A.; Hartmann, M. J.; Crawford, S. E.; Kozycz, L. M.; Seferos, D. S.; Millstone, J. E. Quantitative Analysis of Thiolated Ligand Exchange on Gold Nanoparticles Monitored by 1H NMR Spectroscopy. *Anal. Chem.* **2015**, *87* (5), 2771–2778.

(31) Wang, Y.; Bürgi, T. Ligand Exchange Reactions on Thiolate-Protected Gold Nanoclusters. *Nanoscale Adv.* **2021**, *3* (10), 2710–2727.

(32) Goldmann, C.; Ribot, F.; Peiretti, L. F.; Quaino, P.; Tielens, F.; Sanchez, C.; Chanéac, C.; Portehault, D. Quantified Binding Scale of Competing Ligands at the Surface of Gold Nanoparticles: The Role of Entropy and Intermolecular Forces. *Small* **2017**, *13* (20).

(33) Srisombat, L.; Jamison, A. C.; Lee, T. R. Stability: A Key Issue for Self-Assembled Monolayers on Gold as Thin-Film Coatings and Nanoparticle Protectants. *Colloids Surfaces A Physicochem. Eng. Asp.* **2011**, *390* (1–3), 1–19.

(34) Lee, H. Y.; Shin, S. H. R.; Drews, A. M.; Chirsan, A. M.; Lewis, S. A.; Bishop, K. J. M. Self-Assembly of Nanoparticle Amphiphiles with Adaptive Surface Chemistry. *ACS Nano* **2014**, *8* (10), 9979–9987.

(35) Noh, J.; Kato, H. S.; Kawai, M.; Hara, M. Surface Structure and Interface Dynamics of Alkanethiol Self-Assembled Monolayers on Au(111). *J. Phys. Chem. B* **2006**, *110* (6), 2793–2797.

(36) Xiong, K.; Mitomo, H.; Su, X.; Shi, Y.; Yonamine, Y.; Sato, S.; Ijiro, K. Molecular Configuration-Mediated Thermo-Responsiveness in Oligo(Ethylene Glycol) Derivatives Attached on Gold Nanoparticles. *Nanoscale Adv.* **2021**, *3* (13), 3762–3769.

(37) Oh, E.; Delehanty, J. B.; Sapsford, K. E.; Susumu, K.; Goswami, R.; Blanco-Canosa, J. B.; Dawson, P. E.; Granek, J.; Shoff, M.; Zhang, Q.; et al. Cellular Uptake and Fate of PEGylated Gold Nanoparticles Is Dependent on Both Cell-Penetration Peptides and Particle Size. *ACS Nano* **2011**, *5* (8), 6434–6448.

Chapter 4

Conclusion

In this thesis, I focused on surface modification and investigated the method of precisely control thermo-responsiveness by fair surface modification. In this chapter, I summarize the thesis and afforded the significance and prospects.

In chapter 2, I precisely tuned the assembly temperature (T_A) of AuNPs via surface modification using mixed OEG-alkanethiol ligands to control of terminal hydrophobicity and local OEG density of alkanethiol ligands. Firstly, since this thermo-responsive assembly/disassembly of AuNPs coated with OEG-attached alkanethiols dependent on the hydrophobicity at the terminus, mixing with different hydrophobic terminus at designed ratio is successful to precisely tune the T_A. Then, I confirmed the T_A is curvature-dependent by surface modification using various AuNP sizes and found that the local density of OEG change along with the curvature of AuNPs, suggesting it is in connected with the change in T_A. Importantly, the T_A was also tuned by ligand mixing with a non-thermo-responsive ligand with a shorter OEG chain-length to control the local density of OEG. These results showed tuning of local environment in SAMs by control of mixing ligand ratios is possible to precisely program the surface properties of AuNPs.

In chapter 3, I investigate the ligand exchanged and approached to restrain the biased surface modification. I confirmed the ligand exchange between ligands in high packed SAMs and existing in solution. According to the drastic change and recovery of T_A over time, I inferred that ligand exchange proceeded as ratio of ligands in reaction medium firstly and then showed the unfairness over time on this reaction which is greatly connected to the tiny difference in structures at the terminus and supposed to influence the bias on surface modification. Based on the investigation of ligand exchange, the bias on surface modification was restrained and surface modification proceeded as the mixing

ligand ratios by well-control of modification time and temperature. This finding provides an important reference for surface modification on gold nanoparticles.

In this thesis, I showed the precise control of thermo-responsiveness by fair surface modification. By this method, it is precise and simple to tune T_A of AuNPs to the desired temperature just by surface modification with mixed ligands at a designed ratio . Moreover, a wide range of T_A can be tuned using only two kinds of ligands with tiny differences in structures at the terminus. Importantly, this surface modification is supposed to proceed as the mixing ligand ratio, which is difficult to realize up to now. Although ligand exchange and bias surface modification are complicated and remains unclear, the precise control of thermo-responsiveness by fair surface modification have been realized, which is a positive step to approach to bio-application for tumor-targeted photothermal cancer therapy. In future, the ligand exchange will be investigated in depth by mathematical analysis and molecular dynamic simulation to provide visual data that help design and enhance the controllability of this system. In addition, thermo-responsiveness in cell and mouse experiment are expected to be prepared for bio-application in vivo. I believe that these studies have contributions to the development of photothermal cancer therapy.

Acknowledgement

These studies presented in this thesis have been performed under the guide of Prof. Kuniharu Ijiro. I would like to express my sincerest gratitude for his invaluable guidance and continuous encouragement throughout these studies.

I gratefully appreciate to Associate Prof. Hideyuki Mitomo, Assistant Prof. Yusuke Yonamine (Research Institute for Electronic Science, Hokkaido University) for their kind and valuable guidance to my research.

I am deeply grateful to Prof. Nobuyuki Tamaoki (Research Institute for Electronic Science, Hokkaido University), Prof. Takayuki Kurokawa (Faculty of Science, Hokkaido University), for valuable guidance and suggestion to summarize this thesis.

I wish to thank Dr. Mba Joshua Chidiebere, Dr. Yu Sekizawa, Dr.Han Lin, Dr. Melda Taspika, Dr. Jingyan Yang, Dr.Yali Shi, Dr. Ryo Sugiyama, Dr. Wenting Wei, Dr. Zhiyu He, Ms. Chisato Toyokawa, Mr. Zirui Jiang, Mr. Wei Jie Cheah, Mr.Yingqi Mu, Mr. Tianxu Gao, Ms. Honoka Niwa, Ms. Yuka Hasekawa, Mr. Kaito Shishido, Mr. Yuusei Miyada, Ms. Honoka Watanabe, Ms. Hono Ogihara, Ms. Aki Okuhara, Ms. Chie Takeuchi for their hospital support during my laboratory life in Molecular Device Laboratory.

This work was supported by JST SPRING, Grant Number JPMJSP2119.

Finally, I would like to express my special thanks to my family and friends for their hearty encouragement and assistance.

Kun Xiong